AFOSR TR 59-122

THE UNIVERSITY OF MICHIGAN
COLLEGE OF LITERATURE, SCIENCE, AND THE ARTS
Department of Physics

Final Report

PART I. GALVANO-MAGNETIC EFFECTS

W. Tantraporn

Ernst Katz
Project Supervisor

UMRI Project 2613

under contract with:

UNITED STATES AIR FORCE
AIR RESEARCH AND DEVELOPMENT COMMAND
OFFICE OF SCIENTIFIC RESEARCH, SOLID STATE SCIENCES DIVISION
CONTRACT NO. AF 49(638)-69, PROJECT NO. 19751
WASHINGTON, D.C.

administered by:

THE UNIVERSITY OF MICHIGAN RESEARCH INSTITUTE ANN ARBOR

August 1959

TABLE OF CONTENTS

LIST OF TABLES

LIST OF FIGURES

ABSTRACTS

PART I. GALVANO-MAGNETIC EFFECTS

A historical preface is given. In Section 2 the phenomenological theory as developed by Kao and Katz is summarized, with special emphasis on applications to bismuth and gallium. In Section 3 the experimental method of measurement and results for bismuth are described. It is found that all resistivity brackets can be represented by the formula $\{\ \} = \Gamma_o T e^{-\beta\sqrt{T}}$, where Γ_o is a constant, different for each bracket and β depends almost exclusively on the order of the bracket. This dependence is roughly given by $\beta_n = 2n/(n+4)$. No theoretical interpretation of these results is presently available. Their compatibility with current models of the energy surfaces of electrons and holes in bismuth is being tested. The amount of labor involved in this testing has precluded our reaching a definite conclusion at the time of this writing. The question will be pursued further. In Section 4 results from the literature for gallium are analyzed in terms of our phenomenological constants. Here also relations of the above form hold. Again the electron theoretical implications remain to be worked out. In Section 5 the procedure of testing and its complications are sketched, as is the direction in which an entire new series of bracket relations is in process of being discovered by the present analysis.

PART II. THE PHOTOGRAPHIC SEQUENCE EFFECT

In Section 1 the motivation of this study is given: comparison of limiting low-intensity reciprocity failure slope from sequence loops with direct measurements by Martin, and study of the number of quanta active in the formation of a just developable latent image as a function of grain size, density, and type of development by means of sequence loops. In Section 2 the method of sequence exposures is briefly described experimentally and theoretically and the experimental results are described. These were obtained with Eastman Kodak type 33 emulsions and with a set of emulsions, kindly supplied especially for this study by Eastman Kodak laboratories, consisting of nonsensitized pure AgBr emulsions of different average grain sizes. The results confirm qualitatively the trend of the theoretical work but lead to quantitative difficulties, which are discussed in Section 3. The conclusions are summarized in Section 4. At present no practical way is seen to refine the theory to a degree that would make for its quantitative applicability. To do so would require introducing too large a number of unknown parameters and make it very complex. For qualitative use the theory and the method of sequence-loop studies seem useful tools for the determination of the number of quanta that are involved in the formation of one just developable speck. Values in the range 3 to 20 quanta were found in the present studies. This number tends to be lower for grains that require a larger total number of quanta received to become developable, indicating that the efficiency of concentrating the received energy on one speck tends to be lower for grains with smaller just developable specks. No explanation of this trend is presently available.

HISTORICAL PREFACE

The presently terminated contract covers work done during a period of a little over two years. It grew out of work done under several previous contracts starting in 1952 and 1953. To provide a proper perspective of the present work, a brief sketch of its relation to these previous contracts follows.

Contract No. DA-20-018-ORD-12258 with the Office of Ordnance Research of the U. S. Army was initiated in 1952 for research on "the photographic latent image." Contract No. AF 18(600)-750 with the Office of Scientific Research of the U. S. Air Force was initiated in 1953 for research on "Brillouin Zones." To simplify administration, the first contract was merged with the second early in 1955 at the request of the principal investigator. In 1953, also, Contract No. DA-36-039-SC-52601 with the Signal Corps Engineering Laboratories at Fort Monmouth was initiated for research on "galvano-magnetic effects." It was terminated in the summer of 1956 and its function was integrated with the Air Force contract into the present instrument, Contract No. AF-49(638)-69, initiated for "Solid-State Research" in November, 1956. Meanwhile the work on Brillouin Zones had come to a conclusion, so that the present contract covers, within its general title, work on these two relatively independent branches of solid-state physics: "galvano-magnetic effects," and "the photographic latent image." For this reason the final report consists of two separate parts, probably of interest to different readers.

The study of Brillouin Zones led to the Ph.D. thesis of Dr. G. B. Spence[1] in 1956. Dr. Spence was swamped with work at the position he accepted, and a series of health problems arose in his family, so no publication of his work has yet appeared. The results are, however, available in report form.

The study of the galvano-magnetic effects led to the Ph.D. theses of Dr. L. P. Kao[2] in 1956 and Dr. W. Tantraporn[3] in 1958. A paper of Kao's results was published.[4] A paper of Tantraporn's results is in preparation and will be submitted for publication in the near future. Its contents are mainly a condensed version of Part I of this final report.

The study of the photographic latent image led to the Ph.D. thesis of Dr. R. L. Martin[5] in 1956. The results have not been published in journals for reasons similar to those of Dr. Spence. As a further result of work on the photographic latent image, a paper was published by Dr. J. Enns, research physicist with this contract, and E. Katz.[6] The experiments were carried out by Dr. Enns. Another paper is in preparation and will be submitted for publication in the future. Its contents will correspond to Part II of this final report.

At various scientific meetings six papers[7] were read to communicate the results of this research. In addition to the physicists mentioned, about a dozen students were employed part-time for various periods to assist with various phases of the work. Most of them were graduate students in physics, and their experience during these periods may be considered of value toward their education as physicists.

PART I. GALVANO-MAGNETIC EFFECTS

1. Introduction

The results of the work on galvano-magnetic effects fall into three stages.

At the first stage the phenomenological theory is developed. The manner in which crystal symmetry, electrode geometry, and magnetic field strength and orientation influence the galvano-magnetic measurements is clarified. This theory, which is necessary for any proper description and organization of such measurements, is described in detail in the thesis of L. P. Kao.[2] A paper by L. P. Kao and E. Katz[4] summarizes the results. For the sake of brevity, the proofs of many statements in the paper are left to the reader; these can all be found in the above thesis. For a proper understanding of our notation and our procedure of measurement, it is necessary to outline some of the results of the phenomenological theory. This will be done in Section 2.

At the second stage, measurements are made on bismuth single crystals as a function of the temperature between 120°K and room temperature. Also, measurements on gallium from the literature[8] are analyzed in terms of the proper galvano-magnetic constants. The results of W. Tantraporn's thesis for bismuth have been amplified and are reported in Section 3 for the first time. The reinterpretation of Blom's data on gallium is given in Section 4.

At the third stage an interpretation of the measurements is attempted in terms of the electron theory. Some new relations are developed. This work is reported for the first time in Section 5.

* * *

The purpose guiding this work was modified several times during the research. At first the preparation of materials with special galvano-magnetic properties stood in the foreground. It soon became clear that not enough was known about the mechanism underlying the effects so that the work had to become more fundamental and theoretical. It was then realized that the present state of the electron theory was fraught with so many uncertainties that it was found necessary first to develop the phenomenological theory.

The results obtained from our work on the phenomenological theory enabled us, within the limits of available time and manpower, to do the basic measure-

ments for one material, for which bismuth was chosen. Their interpretation in terms of the electron theory became the next goal.

These purposes should be seen against the background of present-day research in the field of electric and magnetic properties of metals and semiconductors. The customary description implies that the shape of the energy surfaces in reciprocal space, especially the shape of the Fermi surface, is fundamental in determining all such properties. However, the inverse question, namely, the obtaining of accurate information concerning the Fermi surface from experimental data, is at present still a basic problem of formidable difficulty. The present research represents some progress toward the solution of this problem, and this aspect constitutes its most important motivation from the standpoint of fundamental research.

2. Phenomenological Theory

2.1. GENERAL

The phenomenological theory as developed by this group has been published[4] but to make this report self-contained, the basic notions and the results for single crystals of gallium and bismuth are sketched briefly here.

In anisotropic materials the electric field vector $\underline{F}$ and the electric current density vector $\underline{J}$ are related by the generalized law of ohm

$$J_i = \sigma_{ij} F_j \qquad (1)$$

The subscripts refer to components relative to a Cartesian system of axes that is most adapted to the symmetry of the material ("symmetry coordinates") and σ_{ij} are the components of the conductivity tensor. The convention of summation over repeated indices is used. The components of the resistivity tensor ρ_{ij} are given in terms of those of the conductivity tensor by

$$\rho_{ij} = \frac{\Delta_{ji}}{\Delta} \qquad (2)$$

where Δ is det σ_{ij}, and Δ_{ji} is cofactor of σ_{ji} in Δ.

The dependence of σ_{ij} (or ρ_{ij}) on an applied magnetic field $\underline{B}$ is called the galvano-magnetic effect. This dependence may be complicated, but as long as (1) holds, Onsager's relations apply:

$$\sigma_{ij}(\underline{B}) = \sigma_{ji}(-\underline{B}) \tag{3}$$

With (2) a relation for the resistivity ρ of the same form as (3) can easily be verified. It is customary to expand $\sigma_{ij}(\underline{B})$ in a three-dimensional Taylor series in powers of the components $B_1B_2B_3$, thus:

$$\sigma_{ij}(\underline{B}) = \sum_{n=o}^{\infty} \sum_{m=o}^{n} \sum_{p=o}^{m} [m-p,p,n-m]_{ij} \, B_1^{m-p} B_2^{p} \, B_3^{n-m} \tag{4}$$

and likewise

$$\rho_{ij}(\underline{B}) = \sum_{n=o}^{\infty} \sum_{m=o}^{n} \sum_{p=o}^{m} \{m-p,p,n-m\}_{ij} \, B_1^{m-p} \, B_2^{p} \, B_3^{n-m} \tag{5}$$

The coefficients, the "brackets," are independent of $\underline{B}$, but depend on the temperature and on the kind of material. For the nth power of $\underline{B}$ there are, to begin with $(n^2 + 3n + 2)9/2$ independent conductivity brackets, and an equal number of resistivity brackets. However, the condition (3) and the symmetry of the crystal impose restrictions which drastically reduce this number.

Onsager's relations (3) imply

$$[m-p,p,n-m]_{ij} = (-)^n \, [m-p,p,n-m]_{ji} \tag{6}$$

Thus, for n even, only ij values 11, 22, 33, 23, 31, 12 need to be considered; for n odd, only 23, 31, 12.

In connection with experimental conditions and the interpretation of measurements, it is desirable to establish the relation between measured quantities and the brackets. If the sample is a single rod-shaped crystal with current flowing in the length direction, it is expedient to introduce a second set of coordinates, "laboratory coordinates," with x^1 along the sample, x^2 in the direction connecting the Hall probes, and x^3 accordingly. Components in the laboratory coordinate system carry superscripts, while those in the symmetry coordinates carry subscripts. One has for the current density $\underline{J}$:

$$J^2 = J^3 = 0$$

The measured quantities are

$$\rho^{\alpha 1} = F^{\alpha}/J^1$$

For $\alpha = 1$ the measurement of the electric field component F^1 along the sample is done by means of two potential probes, called the magneto-resistance probes. For $\alpha = 2$ the measurement of F^2 across the sample is done with two Hall probes. Details of this arrangement are reported in Section 3.

The connection between the measured quantities $\rho^{\alpha 1}$ and the brackets can now easily be established by means of the rules for tensor transformation, and one finds

$$\rho^{\alpha 1} = \ell_i^\alpha \ell_j^1 \rho_{ij} = \sum_{n=0}^{\infty} \sum_{m=0}^{n} \sum_{p=0}^{m} \{m-p, p, n-m\}_{ij} B_1^{m-p} B_2^{p} B_3^{n-m} \ell_i^\alpha \ell_j^1 \qquad (7)$$

Here ℓ_i^α is the direction cosine between the ith symmetry coordinate axis and the αth laboratory coordinate axis. Formula (7) expresses the measured quantity in terms of the material constants, the resistivity brackets. It is clear that the inverse process, expressing the individual brackets in terms of measured quantities, is not a simple matter; the manner in which we have done it will be described in Section 3.

The conventional Hall coefficient $R = F^2/J^1B^3$ is determined by the direction cosines of the laboratory coordinates relative to the symmetry coordinates, and by the first-order brackets ($n = 1$). For example, in an isotropic material $R = \{001\}_{12} = \{010\}_{31} = \{100\}_{23}$. The longitudinal magneto-resistance coefficient is $\{200\}_{11}$, etc.

2.2. BISMUTH

Onsager's relations and the crystal symmetry reduce the number of brackets. For bismuth there are $1/2\ n^2 + 2n + 2$ independent nonvanishing conductivity brackets when n is even, and $1/4\ n^2 + n + 3/4$ when n is odd. Corresponding formulas are found for all other materials (crystal classes).[4] The same numbers hold for resistivity brackets.

Crystal symmetry not only reduces the number of independent brackets but also establishes certain dependences. Table I gives all dependences for $m \leq 6$ for crystals of the group D_{3i} to which bismuth belongs. The trigonal axis is taken along the third symmetry coordinate axis and a binary axis† along the first coordinate axis. An arbitrary even number is designated by e, an arbitrary odd number by o. This table is to be read as follows. If information is desired about a bracket with a given set of values m, p, i, j one may look at the place so designated and find one of three things:

(a) The bracket itself. This is then an independent nonvanishing bracket.

†For an unambiguous definition of a binary axis, see Appendix 1.

TABLE I

BRACKET RELATIONS FOR BISMUTH, D_{3i}

Bracket	ij→	11	22	33	23	31	12
[00·]		$[00e]_{11}$	$[00e]_{11}$	$[00e]_{33}$	0	0	$[00\omega]_{12}$
[10·]		0	0	0	$[01e]_{31}$	$[10\omega]_{31}$	$[10\omega]_{12}$
[01·]		$[10\omega]_{12}$	$-[10\omega]_{12}$	0	$[10\omega]_{31}$	$[01e]_{31}$	0
[20·]		$[20e]_{11}$	$[20e]_{22}$	$[20e]_{33}$	$[20e]_{23}$	$[20\omega]_{31}$	$[20\omega]_{12}$
[11·]		0	0	0	$2[20\omega]_{31}$	$2[20e]_{23}$	$[20e]_{11}-[20e]_{22}$
[02·]		$[20e]_{22}$	$[20e]_{11}$	$[20e]_{33}$	$-[20e]_{23}$	$-[20\omega]_{31}$	$[20\omega]_{12}$
[30·]		0	0	0	$[30e]_{23}$	$[30\omega]_{31}$	$\frac{1}{2}[03\omega]_{11}-\frac{1}{2}[03\omega]_{22}$
[21·]		$-[03\omega]_{11}-2[03\omega]_{22}$	$-2[03\omega]_{11}-[03\omega]_{22}$	$-3[03\omega]_{33}$	$[30\omega]_{31}$	$[30e]_{23}$	$-3[03e]_{12}$
[12·]		0	0	0	$[30e]_{23}$	$[30\omega]_{31}$	$\frac{1}{2}[03\omega]_{11}-\frac{1}{2}[03\omega]_{22}$
[03·]		$[03\omega]_{11}$	$[03\omega]_{22}$	$[03\omega]_{33}$	$[30\omega]_{31}$	$[30e]_{23}$	$[03e]_{12}$
[40·]		$[40e]_{11}$	$-\frac{1}{4}[40e]_{11}+\frac{1}{4}[22e]_{11}+\frac{2}{4}[04e]_{11}$	$[40e]_{33}$	$[40e]_{23}$	$[40\omega]_{31}$	$[40\omega]_{12}$
[31·]		0	0	0	$-[40\omega]_{31}-3[04\omega]_{31}$	$-[40e]_{23}-3[04e]_{23}$	$\frac{1}{2}[40e]_{11}+\frac{1}{2}[22e]_{11}-\frac{3}{2}[04e]_{11}$
[22·]		$[22e]_{11}$	$\frac{3}{2}[40e]_{11}-\frac{1}{2}[22e]_{11}+\frac{2}{2}[04e]_{11}$	$2[40e]_{33}$	$-3[40e]_{23}-3[04e]_{23}$	$-3[40\omega]_{31}-3[04\omega]_{31}$	$2[40\omega]_{12}$
[13·]		0	0	0	$3[40\omega]_{31}+[04\omega]_{31}$	$3[40e]_{23}+[04e]_{23}$	$\frac{3}{2}[40e]_{11}-\frac{1}{2}[22e]_{11}-\frac{1}{2}[04e]_{11}$
[04·]		$[04e]_{11}$	$\frac{3}{4}[40e]_{11}+\frac{1}{4}[22e]_{11}-\frac{1}{4}[04e]_{11}$	$[40e]_{33}$	$[04e]_{23}$	$[04\omega]_{31}$	$[40\omega]_{12}$
[50·]		0	0	0	$[50e]_{23}$	$[50\omega]_{31}$	$[50\omega]_{12}$
[41·]		$-2[50\omega]_{12}-3[05\omega]_{22}$	$-3[05\omega]_{11}-2[50\omega]_{12}$	$-3[05\omega]_{33}$	$-2[50\omega]_{31}+3[05\omega]_{23}$	$-2[50e]_{23}+3[05e]_{31}$	$-3[05e]_{12}$
[32·]		0	0	0	$-4[50e]_{23}+6[05e]_{31}$	$-4[50\omega]_{31}+6[05\omega]_{23}$	$3[05\omega]_{11}-4[50\omega]_{12}-3[05\omega]_{22}$
[23·]		$-3[05\omega]_{11}+6[50\omega]_{12}+[05\omega]_{22}$	$[05\omega]_{11}-6[50\omega]_{12}-3[05\omega]_{22}$	$-2[05\omega]_{33}$	$6[50\omega]_{31}-4[05\omega]_{23}$	$6[50e]_{23}-4[05e]_{31}$	$-2[05e]_{12}$
[14·]		0	0	0	$3[50e]_{23}-2[05e]_{31}$	$3[50\omega]_{31}-2[05\omega]_{23}$	$-[05\omega]_{11}+3[50\omega]_{12}+[05\omega]_{22}$
[05·]		$[05\omega]_{11}$	$[05\omega]_{22}$	$[05\omega]_{33}$	$[05\omega]_{23}$	$[05e]_{31}$	$[05e]_{12}$
[60·]		$[60e]_{11}$	$[60e]_{22}$	$[60e]_{33}$	$[60e]_{23}$	$[60\omega]_{31}$	$[60\omega]_{12}$
[51·]		0	0	0	$-[60\omega]_{31}-3[06\omega]_{31}$	$-[60e]_{23}-3[06e]_{23}$	$-[60e]_{11}+[60e]_{22}-3[06e]_{11}+3[06e]_{22}$
[42·]		$-4[60e]_{11}-2[60e]_{22}+3[06e]_{11}+6[06e]_{22}$	$-2[60e]_{11}-4[60e]_{22}+6[06e]_{11}+3[06e]_{22}$	$-6[60e]_{33}+9[06e]_{33}$	$-2[60e]_{23}-3[06e]_{23}$	$-2[60\omega]_{31}-3[06\omega]_{31}$	$-6[60\omega]_{12}+9[06\omega]_{12}$
[33·]		0	0	0	$2[60\omega]_{31}-2[06\omega]_{31}$	$2[60e]_{23}-2[06e]_{23}$	$2[60e]_{11}-2[60e]_{22}-2[06e]_{11}+2[06e]_{22}$
[24·]		$3[60e]_{11}+6[60e]_{22}-4[06e]_{11}-2[06e]_{22}$	$6[60e]_{11}+3[60e]_{22}-2[06e]_{11}-4[06e]_{22}$	$9[60e]_{33}-6[06e]_{33}$	$-3[60e]_{23}-2[06e]_{23}$	$-3[60\omega]_{31}-2[06\omega]_{31}$	$9[60\omega]_{12}-6[06\omega]_{12}$
[15·]		0	0	0	$3[60\omega]_{31}+[06\omega]_{31}$	$3[60e]_{23}+[06e]_{23}$	$3[60e]_{11}-3[60e]_{22}+[06e]_{11}-[06e]_{22}$
[06·]		$[06e]_{11}$	$[06e]_{22}$	$[06e]_{33}$	$[06e]_{23}$	$[06\omega]_{31}$	$[06\omega]_{12}$

TABLE II

RESISTIVITY BRACKETS OF ORDERS UP TO FOUR EXPRESSED IN TERMS OF CONDUCTIVITY BRACKETS, OR VICE VERSA, IF THE BRACKET NOTATIONS ARE INTERCHANGED
(Independent brackets only are listed.)

n = 0

$$\{000\}_{11} = \frac{1}{[000]_{11}}$$

$$\{000\}_{33} = \frac{1}{[000]_{33}}$$

n = 1

$$\{100\}_{23} = -\frac{[100]_{23}}{[000]_{11}\,[000]_{33}}$$

$$\{001\}_{12} = -\frac{[001]_{12}}{[000]_{11}^{2}}$$

n = 2

$$\{200\}_{11} = -\frac{[200]_{11}}{[000]_{11}^{2}}$$

$$\{200\}_{22} = -\frac{[200]_{22}}{[000]_{11}^{2}} - \frac{[100]_{23}^{2}}{[000]_{11}^{2}\,[000]_{33}}$$

$$\{200\}_{33} = -\frac{[200]_{33}}{[000]_{33}^{2}} - \frac{[100]_{23}^{2}}{[000]_{11}\,[000]_{33}^{2}}$$

$$\{200\}_{23} = -\frac{[200]_{23}}{[000]_{11}\,[000]_{33}}$$

$$\{002\}_{11} = -\frac{[002]_{11}}{[000]_{11}^{2}} - \frac{[001]_{12}^{2}}{[000]_{11}^{3}}$$

$$\{002\}_{33} = -\frac{[002]_{33}}{[000]_{33}^{2}}$$

$$\{011\}_{11} = -\frac{[011]_{11}}{[000]_{11}^{2}}$$

$$\{011\}_{23} = -\frac{[011]_{23}}{[000]_{11}\,[000]_{33}} + \frac{[001]_{12}\,[100]_{23}}{[000]_{11}^{2}\,[000]_{33}}$$

n = 3

$$\{300\}_{23} = -\frac{[300]_{23}}{[000]_{11}\,[000]_{33}} + \frac{[200]_{33}\,[100]_{23}}{[000]_{11}\,[000]_{33}^{2}} + \frac{[200]_{22}\,[100]_{23}}{[000]_{11}^{2}\,[000]_{33}} + \frac{[100]_{23}^{3}}{[000]_{11}^{2}\,[000]_{33}^{2}}$$

$$\{030\}_{12} = -\frac{[030]_{12}}{[000]_{11}^{2}} + \frac{[200]_{23}\,[100]_{23}}{[000]_{11}^{2}\,[000]_{33}}$$

$$\{003\}_{12} = -\frac{[003]_{12}}{[000]_{11}^{2}} + \frac{2\,[001]_{12}\,[002]_{11}}{[000]_{11}^{3}} + \frac{[001]_{12}^{3}}{[000]_{11}^{4}}$$

$$\{021\}_{12} = -\frac{[021]_{12}}{[000]_{11}^{2}} + \frac{[001]_{12}\,([200]_{11} + [200]_{22})}{[000]_{11}^{3}} - \frac{[100]_{23}\,[011]_{23}}{[000]_{11}^{2}\,[000]_{33}} + \frac{[100]_{23}^{2}\,[001]_{12}}{[000]_{11}^{3}\,[000]_{33}}$$

$$\{021\}_{31} = -\frac{[021]_{31}}{[000]_{11}\,[000]_{33}} + \frac{[001]_{12}\,[200]_{23}}{[000]_{11}^{2}\,[000]_{33}} + \frac{[100]_{23}\,[01:]_{11}}{[000]_{11}^{2}\,[000]_{33}}$$

$$\{012\}_{31} = -\frac{[012]_{31}}{[000]_{11}\,[000]_{33}} + \frac{[100]_{23}\,[002]_{33}}{[000]_{11}\,[000]_{33}^{2}} + \frac{[100]_{23}\,[002]_{11}}{[000]_{11}^{2}\,[000]_{33}} - \frac{[001]_{12}\,[011]_{23}}{[000]_{11}^{2}\,[000]_{33}} + \frac{[001]_{12}^{2}\,[100]_{23}}{[000]_{11}^{3}\,[000]_{33}}$$

TABLE II (concluded)

$n = 4$

$$\{400\}_{11} = -\frac{[400]_{11}}{[000]_{11}^2} + \frac{[200]_{11}^2}{[000]_{11}^3}$$

$$\{400\}_{22} = -\frac{[400]_{22}}{[000]_{11}^2} - 2\frac{[300]_{23}[100]_{23}}{[000]_{11}^2[000]_{33}} + \frac{[200]_{22}^2}{[000]_{11}^3} + \frac{[200]_{23}^2}{[000]_{11}^2[000]_{33}} + \frac{[100]_{23}^2[200]_{33}}{[000]_{11}^2[000]_{33}^2} + 2\frac{[100]_{23}^2[200]_{22}}{[000]_{11}^3[000]_{33}} + \frac{[100]_{23}^4}{[000]_{11}^3[000]_{33}^2}$$

$$\{400\}_{33} = -\frac{[400]_{33}}{[000]_{33}^2} - 2\frac{[300]_{23}[100]_{23}}{[000]_{11}[000]_{33}^2} + \frac{[200]_{33}^2}{[000]_{33}^3} + \frac{[200]_{23}^2}{[000]_{11}[000]_{33}^2} + \frac{[100]_{23}^2[200]_{22}}{[000]_{11}^2[000]_{33}^2} + 2\frac{[100]_{23}^2[200]_{33}}{[000]_{11}[000]_{33}^3} + \frac{[100]_{23}^4}{[000]_{11}^2[000]_{33}^3}$$

$$\{400\}_{23} = -\frac{[400]_{23}}{[000]_{11}[000]_{33}} + \frac{[200]_{23}[200]_{22}}{[000]_{11}^2[000]_{33}} + \frac{[200]_{23}[200]_{33}}{[000]_{11}[000]_{33}^2} + \frac{[100]_{23}^2[200]_{23}}{[000]_{11}^2[000]_{33}^2}$$

$$\{040\}_{11} = -\frac{[040]_{11}}{[000]_{11}^2} - 2\frac{[300]_{23}[100]_{23}}{[000]_{11}^2[000]_{33}} + \frac{[200]_{22}^2}{[000]_{11}^3} + \frac{[100]_{23}^2[200]_{33}}{[000]_{11}^2[000]_{33}} + 2\frac{[100]_{23}^2[200]_{22}}{[000]_{11}^3[000]_{33}} + \frac{[100]_{23}^4}{[000]_{11}^3[000]_{33}^2}$$

$$\{040\}_{23} = -\frac{[040]_{23}}{[000]_{11}[000]_{33}} + \frac{[030]_{12}[100]_{23}}{[000]_{11}^2[000]_{33}} - \frac{[200]_{23}[200]_{11}}{[000]_{11}^2[000]_{33}} - \frac{[200]_{23}[200]_{33}}{[000]_{11}[000]_{33}^2} - \frac{[100]_{23}^2[200]_{23}}{[000]_{11}^2[000]_{33}^2}$$

$$\{004\}_{11} = -\frac{[004]_{11}}{[000]_{11}^2} - 2\frac{[003]_{12}[001]_{12}}{[000]_{11}^3} + \frac{[002]_{11}^2}{[000]_{11}^3} + 3\frac{[001]_{12}^2[002]_{11}}{[000]_{11}^4} + \frac{[001]_{12}^4}{[000]_{11}^5}$$

$$\{004\}_{33} = -\frac{[004]_{33}}{[000]_{33}^2} + \frac{[002]_{33}^2}{[000]_{33}^3}$$

$$\{301\}_{12} = -\frac{[301]_{12}}{[000]_{11}^2} + \frac{[011]_{23}([200]_{23} - [200]_{33})}{[000]_{11}^2[000]_{33}} + \frac{[011]_{11}}{[000]_{11}^3}\left([200]_{11} + [200]_{22} + \frac{[000]_{11}}{[000]_{33}}[200]_{33} + \frac{[100]_{23}^2}{[000]_{33}}\right)$$

$$\{031\}_{11} = -\frac{[031]_{11}}{[000]_{11}^2} - 2\frac{[030]_{12}[000]_{12}}{[000]_{11}^3} - 2\frac{[021]_{31}[100]_{23}}{[000]_{11}^2[000]_{33}} + 2\frac{[011]_{11}}{[000]_{11}^3}\left([200]_{22} + \frac{[100]_{23}^2}{[000]_{33}}\right) + 2\frac{[200]_{23}[100]_{23}[001]_{12}}{[000]_{11}^3[000]_{33}}$$

$$\{031\}_{33} = -\frac{[031]_{33}}{[000]_{33}^2} - 2\frac{[021]_{31}[100]_{23}}{[000]_{11}[000]_{33}^2} - 2\frac{[200]_{23}[011]_{23}}{[000]_{11}[000]_{33}^2} + 2\frac{[200]_{23}[100]_{23}[001]_{12}}{[000]_{11}^3[000]_{33}} + \frac{[011]_{11}[100]_{23}^2}{[000]_{11}^2[000]_{33}^2}$$

$$\{031\}_{23} = -\frac{[031]_{23}}{[000]_{11}[000]_{33}} + \frac{([300]_{23}[001]_{12} + [021]_{12}[100]_{23})}{[000]_{11}^2[000]_{33}} + \frac{[200]_{23}[011]_{11}}{[000]_{11}^2[000]_{33}} - \left(\frac{[200]_{33}}{[000]_{33}} + \frac{[200]_{11}}{[000]_{11}} + \frac{[011]_{23}^2}{[000]_{11}[000]_{33}}\right) \times$$

$$\left(\frac{[001]_{12}[100]_{23}}{[000]_{11}^2[000]_{33}} - \frac{[011]_{23}}{[000]_{11}[000]_{33}}\right)$$

$$\{202\}_{11} = -\frac{[202]_{11}}{[000]_{11}^2} - 2\frac{[021]_{12}[001]_{12}}{[000]_{11}^3} + \frac{[011]_{11}^2 + 2[200]_{11}[002]_{11}}{[000]_{11}^3} + \frac{[011]_{23}^2}{[000]_{11}^2[000]_{33}} - 2\frac{[011]_{23}[100]_{23}[001]_{12}}{[000]_{11}^3[000]_{33}} + \frac{[001]_{12}^2}{[000]_{11}^4}(2[200]_{11} + [200]_{22})$$

$$+ \frac{[001]_{12}^2[100]_{23}^2}{[000]_{11}^4[000]_{33}}$$

$$\{202\}_{22} = -\frac{[202]_{22}}{[000]_{11}^2} - 2\frac{[012]_{31}[100]_{23}}{[000]_{11}^2[000]_{33}} - 2\frac{[021]_{12}[001]_{12}}{[000]_{11}^3} + \frac{[011]_{11}^2 + 2[002]_{11}[200]_{22}}{[000]_{11}^3} + \frac{[002]_{33}[100]_{23}^2}{[000]_{11}^2[000]_{33}^2} + 2\frac{[002]_{11}[100]_{23}^2}{[000]_{11}^3[000]_{33}}$$

$$- 2\frac{[011]_{23}[100]_{23}[001]_{12}}{[000]_{11}^3[000]_{33}} + \frac{[001]_{12}^2}{[000]_{11}^4}([200]_{11} + 2[200]_{22}) + 2\frac{[100]_{23}^2[001]_{12}^2}{[000]_{11}^4[000]_{33}}$$

$$\{202\}_{33} = -\frac{[202]_{33}}{[000]_{33}^2} - 2\frac{[012]_{31}[100]_{23}}{[000]_{11}[000]_{33}^2} + 2\frac{[200]_{33}[002]_{33}}{[000]_{33}^3} + \frac{[011]_{23}^2}{[000]_{11}[000]_{33}^2} + \frac{[100]_{23}^2[002]_{11}^2}{[000]_{11}^2[000]_{33}^2} + 2\frac{[100]_{23}^2[002]_{33}}{[000]_{11}[000]_{33}^3}$$

$$+ \frac{[001]_{12}^2}{[000]_{11}^2[000]_{33}^2}([200]_{33} - [200]_{23}) - 2\frac{[011]_{23}[100]_{23}[001]_{12}}{[000]_{11}^2[000]_{33}^2} + \frac{[100]_{23}^2[001]_{12}^2}{[000]_{11}^3[000]_{33}^2}$$

$$\{202\}_{23} = -\frac{[202]_{23}}{[000]_{11}[000]_{33}} + \frac{1}{[000]_{11}[000]_{33}}(-[021]_{31}[001]_{12} + [200]_{23}[002]_{11} + [011]_{11}[011]_{23}) + \frac{[200]_{23}}{[000]_{11}^2[000]_{33}}\left(2[002]_{11} + \frac{[000]_{11}}{[000]_{33}}[002]_{33} + \frac{[001]_{12}^2}{[000]_{11}}\right)$$

$$\{013\}_{11} = -\frac{[013]_{11}}{[000]_{11}^2} + 2\frac{[002]_{11}[011]_{11}}{[000]_{11}^3} + \frac{[011]_{11}[001]_{12}^2}{[000]_{11}^4}$$

$$\{013\}_{23} = -\frac{[013]_{23}}{[000]_{11}[000]_{33}} + \frac{[003]_{12}[100]_{23}}{[000]_{11}^2[000]_{33}} + \frac{[021]_{31}[001]_{12}}{[000]_{11}^2[000]_{33}} - \frac{[002]_{11}[011]_{23}}{[000]_{11}^2[000]_{33}} + \left(\frac{[011]_{23}}{[000]_{11}[000]_{33}} - \frac{[100]_{23}[001]_{12}}{[000]_{11}^2[000]_{33}}\right)\left(2\frac{[002]_{11}}{[000]_{11}} + \frac{[002]_{33}}{[000]_{33}} + \frac{[001]_{12}^2}{[000]_{11}^2}\right)$$

Note: The n = 4 part of this table has been checked 3 times. Some errors were found during the first 2 times but the third check found no errors. The table now is probably correct, but more errors could be possible, though very unlikely.

(b) A different independent bracket or a linear combination of several independent brackets, with an (n-m) value of the same parity as the given bracket. The given bracket is then equal to what is found there.

(c) Zero, or a different independent bracket or a linear combination of independent brackets with an (n-m) value of different parity as the given bracket. The given bracket vanishes.

For example, $[221]_{12} = 2[401]_{12}$ according to (b), while $[222]_{12} = 0$ according to (c).

The same table is valid for curly (resistivity) brackets. According to (2), (4), and (5) it is possible to express resistivity and conductivity brackets in terms of each other. The relations up to n = 4 are given for bismuth explicitly in Table II, expressing resistivity brackets in terms of conductivity brackets. The same table can be used to express conductivity brackets in terms of resistivity brackets by simply interchanging { } and [ ].

2.3. GALLIUM

For gallium there are $3/4\ n^2 + 3n + 3$ independent nonvanishing conductivity brackets when n is even and $3/8\ n^2 + 3/2\ n + 9/8$ when n is odd. The same numbers apply to resistivity brackets.

Table III gives all nonvanishing brackets for crystals of the class D_2, to which gallium belongs. They are all independent. The same table holds for resistivity brackets.

TABLE III

NONVANISHING INDEPENDENT BRACKETS FOR GALLIUM, D_2

ij	11	22	33	23	31	12
Bracket	[eee]	[eee]	[eee]	[eωω]	[ωeω]	[ωωe]
				[ωee]	[eωe]	[eeω]

The relations between conductivity and resistivity brackets will not be used. Tables for conversion can be found in Ref. 2 if needed.

* * *

3. Experimental Determination of Galvano-Magnetic Constants for Bismuth

3.1. PURPOSE

The purpose of this work is to determine the galvano-magnetic constants, to as high an order n as is experimentally feasible, as a function of the tem-

perature. Practical limitations permitted the determination of all constants (resistivity brackets) for $n \leq 4$ and a few up to $n = 6$, in the temperature range 120°K - 300°K for bismuth. Particular stress was laid on obtaining data at small temperature steps.

3.2. METHOD

The general features of the method are described here. For details the reader is referred to Tantraporn.[3] Rod-shaped single crystals of pure bismuth were grown with crystal axes oriented as required. They were furnished with current leads, a pair of magneto-resistance probes, and a pair of Hall probes. The signals of these probes were amplified and recorded, while the sample, being mounted in a kind of Cardan suspension in a temperature bath, was moved in and out of the magnetic field of desired strength. Thus the experimental independent variables were:

(a) the direction of the rod (current) with respect to the crystal axes,

(b) the direction of the Hall probes with respect to the crystal axes,

(c) the orientation of the magnetic field with respect to the crystal axes,

(d) the intensity of the magnetic field, and

(e) the temperature.

A method was designed so as to cover adequately the influence of all these variables. Rather than aiming for a strict minimum of the number of measurements, the procedure was planned to afford a considerable amount of self-checking of the data (see Appendix 3), and continuous recording of some variables as a further precaution. Thus we feel that the results presented in this report possess a considerable degree of reliability. For details of the methods used for self-checking, the reader is referred to Tantraporn.[3] The main features will now be described.

3.3. CRYSTALS

The bismuth used was obtained from the American Smelting and Refining Co., with a stated purity of 99.99+%. After a few zone-melting passes, the middle part of the ingot was used for the preparation of single crystals.

Three single crystals were grown for the purpose of our measurements from oriented seeds inside pyrex tubing. The crystals were cylinders of about 0.2 cm diameter and 3 cm length. Their crystallographic axes were oriented as follows, as determined by optical measurements of cleavage planes and slip lines.

TABLE IV

SAMPLE SPECIFICATIONS

Sample	Θ	κ
A	0	-
B	90°	$90° \pm k.120°$
C	45°	$0° \pm k.120°$

Here Θ is the angle between the trigonal axis and the rod, and κ is the angle between a binary axis and the normal of the plane containing the trigonal axis and the rod. The angles were determined with an error of less than 1°. (For an unambiguous definition of the binary axis, see Appendix 1, where it is shown that, of the two opposite directions along each binary axis, a definite one should be chosen as the positive direction. If the other is chosen as the positive direction, a number of brackets—marked with an asterisk in Table VIII—must receive a minus sign.)

3.4. MOUNTING OF SAMPLES, TEMPERATURE CONTROL, MAGNET

Current leads were fused to the ends of the bismuth rod. Magneto-resistance (voltage) probes consisted of sharp bronze points pushed lightly against the crystal by small bronze springs. The Hall probes were two straight, parallel, bronze wires, touching the sample at two ends of its diameter like brushes, permitting rotation of the sample around its own longitudinal axis. The sample plus probes and leads was mounted in a special sample holder, permitting rotation of the sample about three axes independently (see Fig. 1). The three angles ϕ, ψ, and α associated with these rotations are defined in Appendix 2. The ϕ rotation was motor driven at a slow rate of one revolution in about 4.5 min, clockwise and counterclockwise. The two senses allow the elimination of any emf due to the rotation in the magnetic field ("dynamo effect"). For each ϕ run, the angles ψ and α were set at a fixed value by means of suitable gears, manipulated from outside of the clear Dewar thermostat in which the sample plus holder were immersed.

The clear Dewar permitted a visual check on the scales of the sample holder of the values at which ψ and α were set. The Dewar was filled with isopentane as thermostatic fluid. By running liquid nitrogen through a copper spiral that was also immersed with the sample holder (see the top of Fig. 1), the thermostatic fluid plus sample holder were precooled to 121°K, the melting point of isopentane. The process of warming up was so slow that the temperature of the sample could be considered constant during one measurement, that is, one continuous recording as a function of ϕ for a fixed setting of ψ and α, inside and outside of the magnetic field. In the course of a day, the temperature gradually

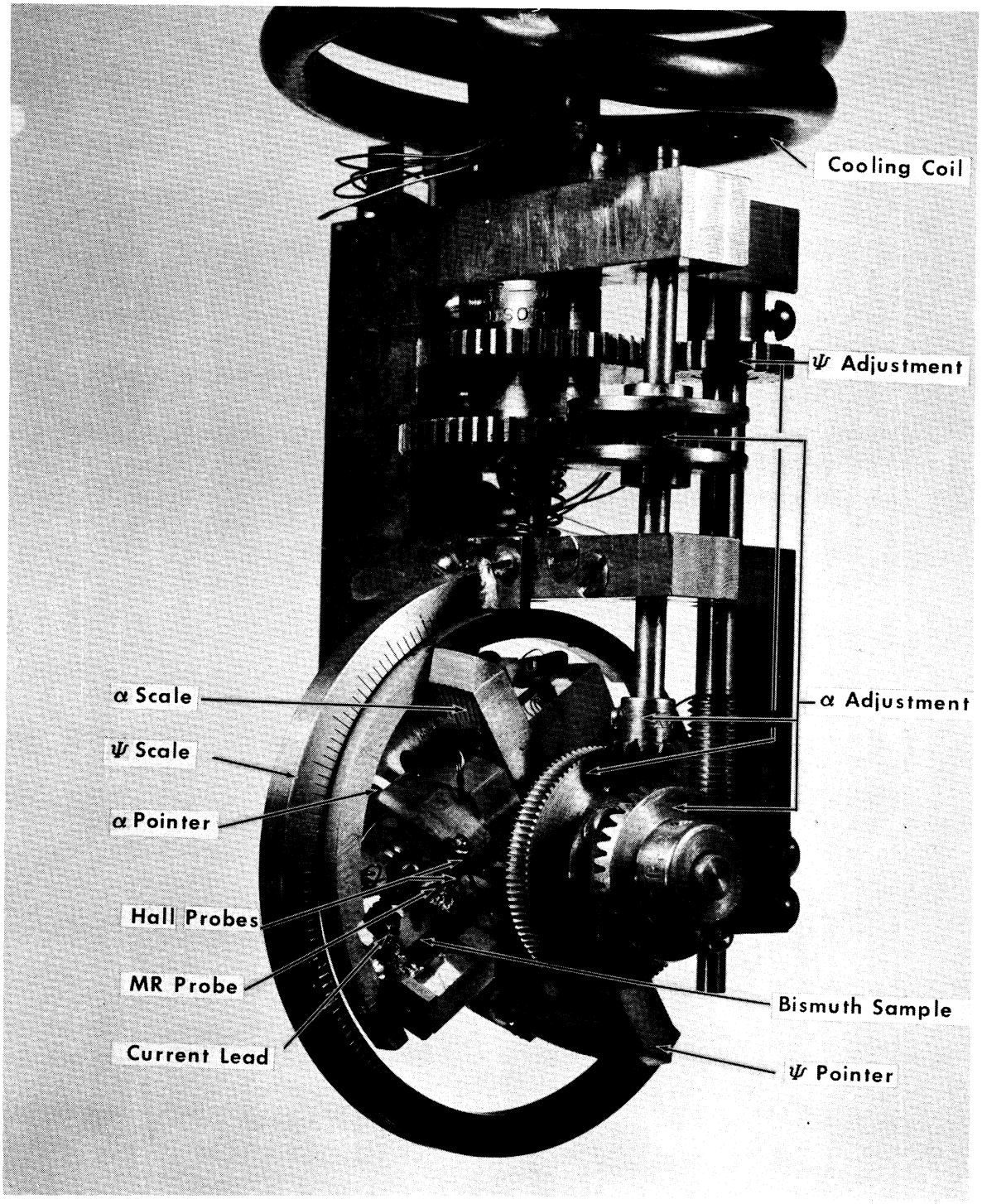

Fig. 1. The sample in the sample holder.

climbed to room temperature and measurements were taken at temperature intervals of about 15°. The temperature of the sample was determined continuously by a copper constantan thermocouple with a potentiometer. One junction was fused into the bismuth crystal at a current probe contact, the other junction was held at 0°C.

A horizontal permanent C-magnet with additional energizing coils provided the magnetic field. The gap was 9.8 cm between pole faces of 17-cm diameter. The value of the magnetic field was set by a current through the energizing coils, and was held constant permanently by packs of Alnico rods behind the pole pieces after the current was switched off. The maximum permanent field retainable in this way was about 1200 gauss with a nonuniformity of less than 0.5% within a spherical volume of radius 3 cm around the center of the gap. The value of the field was determined accurately by the proton resonance technique. The Dewar containing the sample with all accessories was mounted on a carriage which could be moved in and out of the gap manually.

The voltage between the potential probes was balanced by means of a potentiometer circuit, and the change in the voltage due to moving the sample in and out of the magnetic field was fed to a Leeds and Northrup recorder through a d-c converter-amplifier. The smallest signal that could be detected, limited by noise, was 2×10^{-8} v.

3.5. PROCEDURE FOR SEPARATION OF BRACKETS

The voltages measured at any given temperature by the probes as described, when the sample is moved into and out of the magnetic field, are in general linear combinations of brackets, whose coefficients depend on the magnitude and direction of the magnetic field with repsect to the crystal axes, and on the orientation of the electrodes with respect to the crystal axes. To separate the individual brackets, various measurements must be combined.

The relation between the quantity $\rho^{\alpha 1}$, measured by the probes, and the magnetic field $\underline{B}$ is given by Eq. (7). For $B \leq 1200$ gauss and $T > 120°K$, brackets up to $n = 4$ were found adequate to describe almost all the measurements. The separation of the brackets can be performed in the following five steps, which aim to establish conditions under which the right-hand side of Eq. (7) will become as simple as possible.

(a) Measurement of Even and Odd Bracket Combinations.—From the work of Kao and Katz,[4] it is clear that the right side of (7) contains only brackets with even n if $\alpha = 1$ (magneto-resistance measurements), or only brackets with odd n if $\ell_i^1 = 1$, $B_1 = 0$ (Hall measurements on sample B with transverse $\underline{B}$).

(b) Sample Choice for Simple Bracket Combinations.—Referring again to Eq. (7), it can be seen that the number of brackets involved in each measurement can be cut down by special conditions on $\ell_i^{\alpha} \ell_j^1$, implying the use of proper samples. The samples A, B, C described in Table IV were chosen as being the most favorable in this respect.

(c) Settings of α, ψ for Simple Bracket Combinations.—Briefly, α is the angle between the line connecting the Hall probes and the normal to the plane through the trigonal axis and the length direction of the sample; ψ is the angle between the length direction of the sample and the downward vertical. For more complete details regarding these definitions, especially which sense to take as positive, see Appendix 2.

By choosing special settings of the angles α and ψ, one can impose special conditions on the direction cosines γ_i of the magnetic field $\underline{B}$ with respect to the crystal axis, and thus reduce the number of brackets involved in Eq. (7) with nonvanishing coefficients. These settings are defined in Table V. Their effects on γ_i follow from the formulas given in Appendix 2 and are also briefly listed in Table V. The choice of a given sample and a given setting fixes θ, κ, α, and ψ but leaves the rotation of the sample about the vertical ϕ axis still free.

TABLE V

SETTING SPECIFICATIONS

Setting	α	ψ	Implications
1	0	0	$\gamma_3 = 0$ for all samples
2	0	$\theta - \pi/2$	$\gamma_1 = 0$ for samples A, B; $\gamma_2 = 0$ for C
3	0	$\theta + \pi/4$	Some $\gamma_i\gamma_j$ products are equal
4	$-\pi/2$	$\pi/2$	$\gamma_2 = 0$ for B; $\gamma_1 = 0$ for C
5	$-\pi/2$	0	$\gamma_1 = 0$ for B

(d) Harmonic Analysis of ϕ Dependence.—For given samples and settings the only remaining degree of freedom is the rotation about the vertical ϕ axis. When the sample was rotated slowly by a synchronous motor and reduction gear combination in the horizontal magnetic field $\underline{B}$, the recorder trace of the change of voltage as a function of ϕ can be represented for the magneto-resistance probes by

$$\rho^{11} = C_0 + C_2 \cos 2(\phi-\phi_2) + C_4 \cos 4(\phi-\phi_4) \quad \ldots \qquad (8)$$

and for the Hall probes by

$$\rho^{21} = C_1 \cos (\phi-\phi_1) + C_3 \cos 3(\phi-\phi_3) \quad \ldots \qquad (9)$$

The coefficients of cos $n\phi$ and sin $n\phi$ in these expressions are $C_n \cos n\phi_n$ and

$C_n \sin n\phi_n$, respectively. Thus C_n and ϕ_n can be determined from a harmonic analysis of the recorder traces of ρ^{11} and ρ^{21}. Now the right-hand side of (7) can also be expressed in terms of cos $n\phi$, sin $n\phi$, and B. The coefficients are linear combinations of $B^t\{t\}$ where $\{t\}$ represents a bracket of order t of the same parity as n and $n \leq t \leq 4$ (if analysis is carried to fourth order). Conversely, certain simple recurring combinations of $B^t\{t\}$ can be preresented in terms of the coefficients $C_n \cos n\phi_n$ and $C_n \sin n\phi_n$ as shown in Tables VI and VII. The superprescripts refer to sample and setting as described in Tables IV and V. The expressions given in the right-hand sides of Tables VI and VII suffice for the determination of all brackets up to n = 4. The equations are not unique, since the recordings for the various samples and settings lead to more equations than are given in these tables. The equations given are the most convenient ones and are least subject to experimental error. The remaining ones are used for check relations on the results so obtained (see Appendix 3).

(e) Final Separation of Individual Brackets by B-Variation.—The final separation of the bracket pairs on the left-hand side of the equations in Tables VI and VII is possible by taking measurements at various values of B. The brackets are obtained as intercept and slope of the proper linear plots (right side divided by B^2 or B, versus B^2).

The zeroth order brackets, or usual resistivity components, are obtained conventionally; their measurement will not be discussed here.

* * *

The brackets so obtained refer to one temperature and the whole procedure has to be repeated for each temperature. An example illustrating the way in which this analysis was carried out in practice is given in Appendix 3.

3.6. RESULTS

(a) Manner of Plotting.—From a study of the literature[9] as reported in Ref. 3 it was discovered that extensive material by Blake, van Everdingen, and Okada on the temperature dependence of the galvano-magnetic effect of bismuth appears to fit a rather unconventional formula. The galvano-magnetic effect can be represented by the formula

$$\{\ \} = \Gamma_o T\, e^{-\beta\sqrt{T}} \qquad (10)$$

In other words, a plot of log $1/T\ \{\ \}$ versus $\sqrt{T}$ gives a straight line. Figure 2 shows a few cases. While we have not been able to justify a relation of this kind theoretically, it is quite obvious that more conventional trial functions would show marked deviations from the data. We have therefore plotted our own results in the same way and have found that this manner of plotting is consistent

TABLE VI

EVEN ORDER BRACKETS EXPRESSED IN TERMS OF MEASURED QUANTITIES

1. $B^4 \{400\}_{11} + B^2 \{200\}_{11} = {}^{1B}C_0 - {}^{1B}C_2 \cos 2\,{}^{1B}\phi_2 + {}^{1B}C_4 \cos 4\,{}^{1B}\phi_4$

2. $B^4 \{400\}_{22} + B^2 \{200\}_{22} = {}^{1B}C_0 + {}^{1B}C_2 \cos 2\,{}^{1B}\phi_2 - {}^{1B}C_4 \cos 4\,{}^{1B}\phi_4$

3. $B^4 \{400\}_{33} + B^2 \{200\}_{33} = {}^{2A}C_0 + {}^{2A}C_2 \cos 2\,{}^{2A}\phi_2 + {}^{2A}C_4 \cos 4\,{}^{2A}\phi_4 = {}^{1A}C_0$

4. $B^4 \{400\}_{23} + B^2 \{200\}_{23} = \frac{{}^{1B}C_2}{2} \cos 2\,{}^{1B}\phi_2 - \frac{{}^{1B}C_4}{2} \cos 4\,{}^{1B}\phi_4 - {}^{1C}C_2 \cos 2\,{}^{1C}\phi_2 - {}^{1C}C_4 \cos 4\,{}^{1C}\phi_4$

5. $B^4 \{040\}_{11} + B^2 \{200\}_{22} = {}^{1B}C_0 + {}^{1B}C_2 \cos 2\,{}^{1B}\phi_2 + {}^{1B}C_4 \cos 4\,{}^{1B}\phi_4$

6. $B^4 \{040\}_{23} - B^2 \{200\}_{23} = -\frac{{}^{1B}C_2}{2} \cos 2\,{}^{1B}\phi_2 - \frac{{}^{1B}C_4}{2} \cos 4\,{}^{1B}\phi_4 + {}^{1C}C_2 \cos 2\,{}^{1C}\phi_2 - {}^{1C}C_4 \cos 4\,{}^{1C}\phi_4$

7. $B^4 \{004\}_{11} + B^2 \{002\}_{11} = {}^{2B}C_0 - {}^{2B}C_2 \cos 2\,{}^{2B}\phi_2 + {}^{2B}C_4 \cos 4\,{}^{2B}\phi_4$

8. $B^4 \{004\}_{33} + B^2 \{002\}_{33} = {}^{2A}C_0 - {}^{2A}C_2 \cos 2\,{}^{2A}\phi_2 + {}^{2A}C_4 \cos 4\,{}^{2A}\phi_4$

9. $B^4 \{301\}_{12} + B^2 \{011\}_{11} = 2\,{}^{2B}C_4 \sin 4\,{}^{2B}\phi_4 + 2\sqrt{2}\,{}^{3B}C_2 \sin 2\,{}^{3B}\phi_2$

10. $B^4 \{031\}_{11} + B^2 \{011\}_{11} = 2\,{}^{2B}C_2 \sin 2\,{}^{2B}\phi_2 + 4\,{}^{2B}C_4 \sin 4\,{}^{2B}\phi_4$

11. $B^4 \{031\}_{33} + 0 = 8\sqrt{2}\,{}^{3A}C_2 \sin 2\,{}^{3A}\phi_2 = 4\,{}^{2A}C_2 \sin 2\,{}^{2A}\phi_2 = 8\,{}^{2A}C_4 \sin 4\,{}^{2A}\phi_4$

12. $B^4 \{031\}_{23} + B^2 \{011\}_{23} = -2\,{}^{4C}C_2 \cos 2\,{}^{4C}\phi_2 - 4\,{}^{4C}C_4 \sin 4\,{}^{4C}\phi_4 + \frac{B^4}{2}(\{031\}_{11} + \{031\}_{33}) - \frac{B^2}{2}\{011\}_{11}$

13. $B^4 \{202\}_{11} + B^2(\{200\}_{11} + \{002\}_{11}) = 2\,{}^{4B}C_0 - 6\,{}^{4B}C_4 \cos 4\,{}^{4B}\phi_4$

14. $B^4 \{202\}_{22} + B^2(\{200\}_{22} + \{002\}_{11}) = 2\,{}^{2B}C_0 - 6\,{}^{2B}C_4 \cos 4\,{}^{2B}\phi_4$

15. $B^4 \{202\}_{33} + B^2(\{200\}_{33} + \{002\}_{33}) = 2\,{}^{2A}C_0 - 6\,{}^{2A}C_4 \cos 4\,{}^{2A}\phi_4$

16. $B^4 \{202\}_{23} + B^2 \{200\}_{23} = -{}^{2C}C_0 + 3\,{}^{2C}C_4 \cos 4\,{}^{2C}\phi_4 + \frac{{}^{2A}C_0}{2} - \frac{3\,{}^{2A}C_4}{2} \cos 4\,{}^{2A}\phi_4 + \frac{{}^{2B}C_0}{2} - \frac{3\,{}^{2B}C_4}{2} \cos 4\,{}^{2B}\phi_4$

17. $B^4 \{013\}_{11} + B^2 \{011\}_{11} = 2\,{}^{2B}C_2 \sin 2\,{}^{2B}\phi_2 - 4\,{}^{2B}C_4 \sin 4\,{}^{2B}\phi_4$

18. $B^4 \{013\}_{23} + B^2 \{011\}_{23} = -{}^{4C}C_2 \cos 2\,{}^{4C}\phi_2 + 2\,{}^{4C}C_4 \sin 4\,{}^{4C}\phi_4 + \frac{1}{2}\,{}^{2B}C_2 \sin 2\,{}^{2B}\phi_2 + {}^{2B}C_4 \sin 4\,{}^{2B}\phi_4$

TABLE VII

ODD ORDER BRACKET PAIRS EXPRESSED IN TERMS OF MEASURED QUANTITIES

1. $B^3 \{300\}_{23} + B \{100\}_{23} = {}^{5B}C_1 \sin {}^{5B}\phi_1 - {}^{5B}C_3 \sin 3\,{}^{5B}\phi_3$

2. $B^3 \{030\}_{12} + 0 = \frac{4}{3}\,{}^{2B}C_1 \cos {}^{2B}\phi_1 = 4\,{}^{2B}C_3 \cos 3\,{}^{2B}\phi_3$

3. $B^3 \{003\}_{12} + B \{001\}_{12} = {}^{2B}C_1 \sin {}^{2B}\phi_1 - {}^{2B}C_3 \sin 3\,{}^{2B}\phi_3$

4. $B^3 \{021\}_{31} + 0 = -4\,{}^{5B}C_1 \cos {}^{5B}\phi_1 = 4\,{}^{5B}C_3 \cos 3\,{}^{5B}\phi_3$

5. $B^3 \{021\}_{12} + B \{001\}_{12} = {}^{2B}C_1 \sin {}^{2B}\phi_1 + 3\,{}^{2B}C_3 \sin 3\,{}^{2B}\phi_3$

6. $B^3 \{012\}_{31} + B \{100\}_{23} = {}^{5B}C_1 \sin {}^{5B}\phi_1 + 3\,{}^{5B}C_3 \sin 3\,{}^{5B}\phi_3$

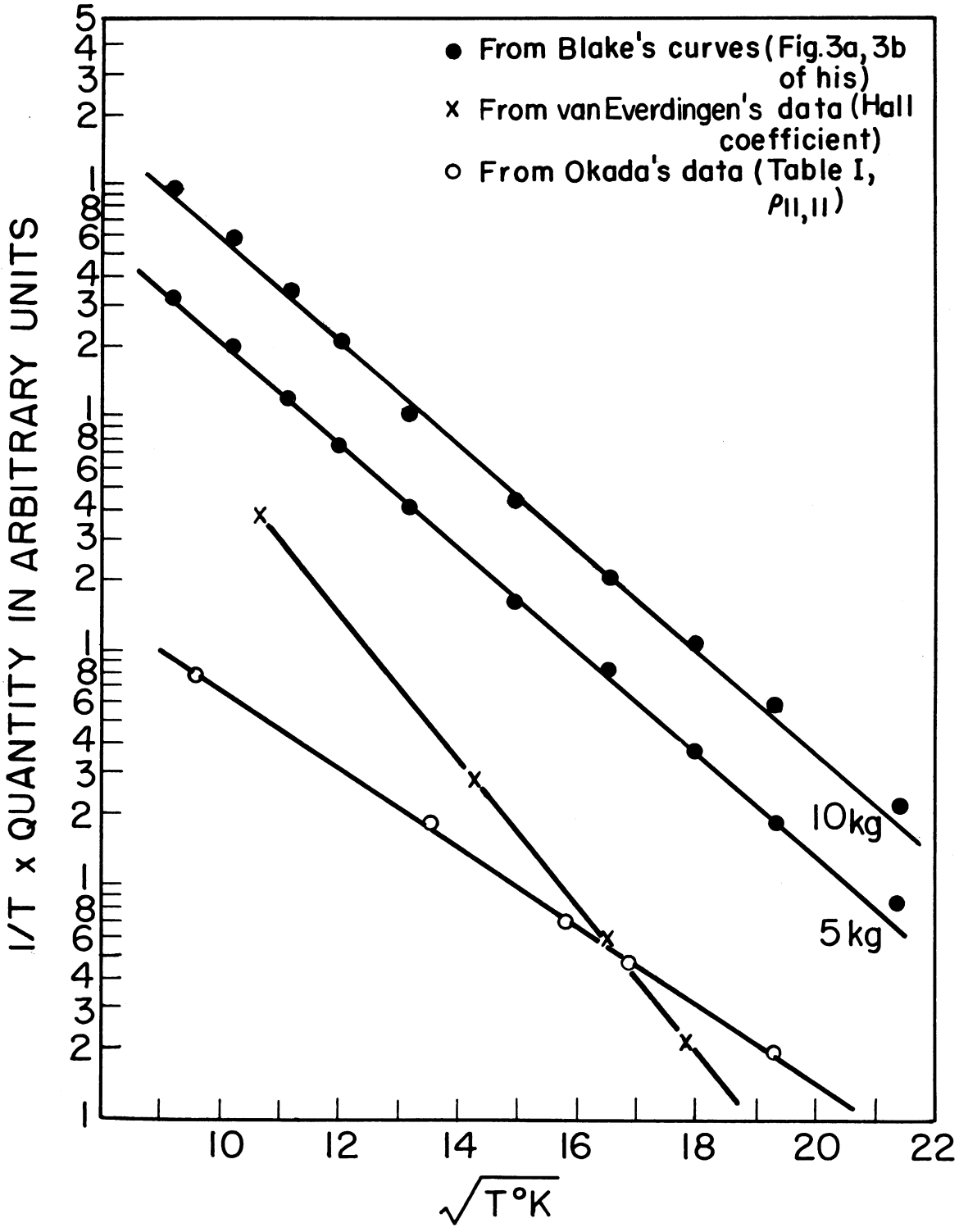

Fig. 2. Galvano-magnetic measurements from the literature plotted according to Equation (10).

with our data throughout. This offers the convenience of allowing us to tabulate our results in very simple form by merely listing two constants, Γ_o and β, for each bracket.

(b) The Measured Zeroth Order Brackets and Their Temperature Dependence.— From the literature it is known that the components of the resistivity tensor without magnetic field (zero-order brackets) vary linearly with the absolute temperature T for pure bismuth. Impurities and structural imperfections are known to cause a change of resistivity which depends nonlinearly on T.[10, 11] The measured resistivities of samples A, B, and C are given in Fig. 3 as a function of T. They correspond to $\{000\}_{33}$, $\{000\}_{11}$, and $1/2\ (\{000\}_{33} + \{000\}_{11})$, respectively. The experimental points of sample A can be fitted by a straight line through T = 0 (dashed line in Fig. 3), while those of B and C must be fitted by curves at lower T. Since they come from the same batch of bismuth and underwent similar treatment, the curvature is more probably due to imperfections rather than impurities. Since the samples show such individual differences, higher-order brackets derived from one sample will be regarded with more confidence than those derived from the combination of data on more than one sample.

(c) The Measured Higher-Order Brackets and Their Temperature Dependence.— All the brackets are found to obey (10) within experimental error for n up to six and T between 121° and room temperature. Therefore we tabulate in Table VIII the constants Γ and β defined by

$$\{\ \} = \Gamma\, T\, e^{-\beta(\sqrt{T}-11)} \qquad (11)$$

where we have introduced for practical convenience:

$$\Gamma = \Gamma_o\, e^{-11\beta} \qquad (12)$$

At the bottom of the table some results are given for n = 5 and 6. These are mostly unresolved combinations of brackets. Their resolution would require many more measurements in all variables. However, they seem to support the general trend of the order of magnitude of Γ and of the dependence of β principally on n only. The results are described by plotting $\log T^{-1}\{\ \}$ vs. $\sqrt{T}$. The slope gives β, the intercept at T = 121° gives Γ, $\Delta\Gamma$ is the region of confidence, and $\Delta\beta$ the difference between the value of β for the best fitting line and the worst line that could be drawn through the experimental points.

(d) Comparison of Our Results with Those of Other Authors.—Figures 4, 5, and 6 show our first- , second- , and third-order data compared with those obtained by Okada[9] and by Abeles and Meiboom.[10] Their data are marked by points at their measuring temperatures. Our data all fall on the lines drawn to represent them. The larger first-order bracket shows good agreement. The other

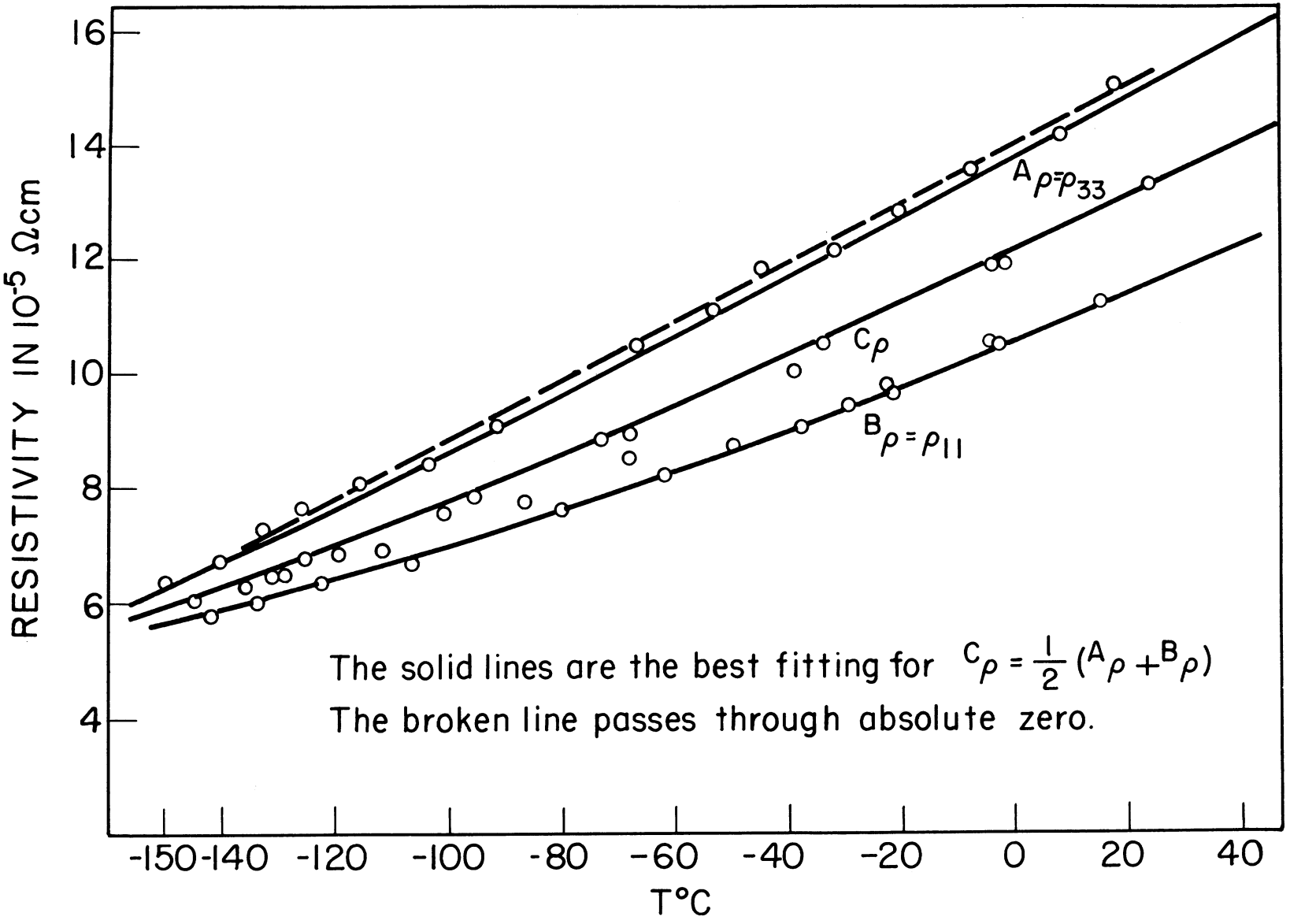

Fig. 3. Resistivity of the samples A, B, and C as a function of temperature.

TABLE VIII

EXPERIMENTAL TEMPERATURE DEPENDENCE OF THE RESISTIVITY BRACKETS OF BISMUTH

$$\{\ \} = \Gamma\ T\ e^{-\beta(\sqrt{T}-11)}$$

n	BRACKET	SAMPLES YIELDING BRACKET	Γ Ωcm/°K GAUSS^n	β $1/\sqrt{°K}$	$\pm\Delta\Gamma$ %	$\pm\Delta\beta$
0	$\{000\}^{(1)}_{11}$	B	3.92 $\times 10^{-7}$	0	2	—
	$\{000\}_{33}$	A	5.10	0	2	—
1	$\{100\}_{23}$	A,B	-4.38 $\times 10^{-10}$	0.38	5	0.01
	$\{001\}^{(2)}_{12}$	—	0.20	0.38	50	0.06
2	$\{200\}_{11}$	B	2.30 $\times 10^{-13}$	0.692	10	0.10
	$\{200\}_{22}$	B	2.70	0.657	10	0.01
	$\{200\}_{33}$	A	2.74	0.60	10	0.005
	$\{200\}^{*}_{23}$	B,C	0.38	0.62	20	0.01
	$\{002\}_{11}$	B	1.15	0.64	10	0.01
	$\{002\}_{33}$	A	0.32	0.625	20	0.01
	$\{011\}^{*}_{11}$	B	1.02	0.72	20	0.02
	$\{011\}_{23}$	B,C	-0.50	0.72	30	0.02
3	$\{300\}_{23}$	B	+1.55 $\times 10^{-16}$	0.988	30	0.03
	$\{030\}^{*}_{12}$	B	-0.26	1.04	50	0.18
	$\lvert\{003\}_{12}\rvert$	B	< 0.02	—	—	—
	$\{021\}^{*}_{31}$	B	+2.25	0.815	30	0.04
	$\lvert\{021\}_{12}\rvert$	B	< 0.02	—	—	—
	$\{012\}_{31}$	B	-0.64	0.575	60	0.1

(1) This fits experimentally only from T = 180°K up (see Fig. 3).

(2) Data from earlier measurements, from T = 170°K up.

* Means bracket changes sign with opposite choice of binary axis (see Appendix 1).

TABLE VIII (Concluded)

n	BRACKET	SAMPLES YIELDING BRACKET	Γ Ω cm/°K GAUSS^n	β $1/\sqrt{°K}$	±ΔΓ %	±Δβ
4	$\{400\}_{11}$	B	-3.0×10^{-19}	1.14	30	0.02
	$\lvert\{400\}_{22}\rvert$	B	< 0.1	—	—	—
	$\{400\}_{33}$	A	−0.49	0.763	30	0.16
	$\{400\}_{23}$	B,C	−0.28	—	100	—
	$\{040\}_{11}$	B	−2.9	1.12	30	0.02
	$\{040\}_{23}$	B,C	−0.28	—	100	—
	$\{004\}_{11}$	B	−0.85	0.81	40	0.08
	$\lvert\{004\}_{33}\rvert$	A	< 0.05	—	—	—
	$\{301\}^*_{12}$	B	+0.1	1.05	60	0.2
	$\{031\}^*_{11}$	B	−3.96	1.14	30	0.03
	$\lvert\{031\}^*_{33}\rvert$	A	< 0.05	—	—	—
	$\{031\}_{23}$	A,B,C	−1.9	1.14	80	0.05
	$\{202\}_{11}$	B	−2.60	1.40	30	0.18
	$\{202\}_{22}$	B	−3.20	1.14	40	0.14
	$\lvert\{202\}_{33}\rvert$	A	< 0.2	—	—	—
	$\{202\}^*_{23}$	A,B,C	−0.8	—	80	—
	$\{013\}^*_{11}$	B	+0.17	1.14	80	0.2
	$\{013\}_{23}$	B,C	−0.04	—	100	—
5	$^{2B}C_5 \sin 5\,^{2B}\phi_5$	B	$+2.95 \times 10^{-23}$	1.06	80	—
	$\lvert^{2B}C_5 \cos 5\,^{2B}\phi_5\rvert$	B	< 0.7	1.06	—	—
6	$\{600\}_{11}$	B	1.5×10^{-25}	1.0	90	0.4
	$^{1B}C_6$	B	2.8×10^{-27}	0.93	70	0.2
	$^{1C}C_6$	C	1.35×10^{-26}	1.2	30	0.1
	$^{3B}C_6 \cos 6\,^{3B}\phi_6$	B	4.3×10^{-27}	1.05	30	0.04
	$\lvert^{3B}C_6 \sin 6\,^{3B}\phi_6\rvert$	B	2.5×10^{-27}	1.05	30	0.04

$$^{2B}C_5 \sin 5\,^{2B}\phi_5 = \tfrac{1}{16}\left(\{005\}_{12} - \{023\}_{12} + \{041\}_{12}\right)$$

$$^{2B}C_5 \cos 5\,^{2B}\phi_5 = \tfrac{1}{16}\left(\{050\}^*_{12} - \{032\}^*_{12}\right)$$

$$^{1B}C_6 = \tfrac{1}{4}\left(\{060\}_{11} + \{060\}_{22} - \{600\}_{11} - \{600\}_{22}\right)$$

$$^{1C}C_6 = -\tfrac{1}{8}\left(\{600\}_{11} + \{600\}_{22} + 2\{600\}_{33} - \{060\}_{11} - \{060\}_{22} - 2\{060\}_{33}\right)$$

$$^{3B}C_6 \cos 6\,^{3B}\phi_6 = \tfrac{1}{32}\left(-\tfrac{21}{8}\{600\}_{11} - \tfrac{7}{2}\{600\}_{22} + \tfrac{15}{4}\{060\}_{11} + \tfrac{5}{2}\{060\}_{22} - \tfrac{7}{8}\{402\}_{11} + \tfrac{1}{4}\{042\}_{11} + \{042\}_{22} - \tfrac{1}{8}\{204\}_{11} + \tfrac{1}{4}\{024\}_{11} - \tfrac{1}{8}\{006\}_{11}\right)$$

$$^{3B}C_6 \sin 6\,^{3B}\phi_6 = \tfrac{1}{32\sqrt{2}}\left(-\tfrac{3}{2}\{051\}_{11} + \tfrac{5}{2}\{501\}_{12} + \tfrac{5}{4}\{051\}_{22} + \tfrac{3}{4}\{033\}_{11} + \tfrac{1}{2}\{033\}_{22} - \tfrac{1}{4}\{015\}_{11}\right).$$

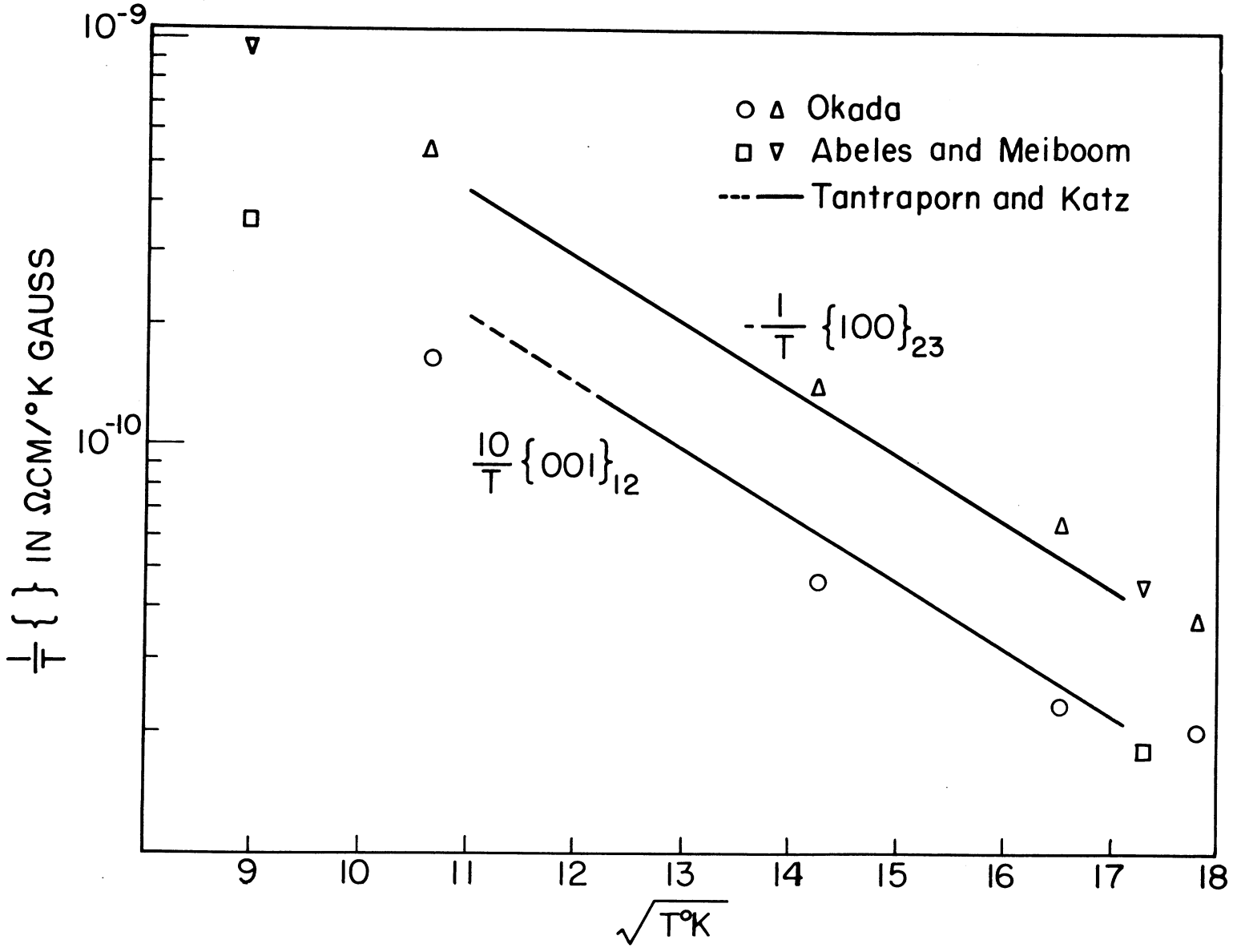

Fig. 4. Comparison of first-order brackets by various authors.

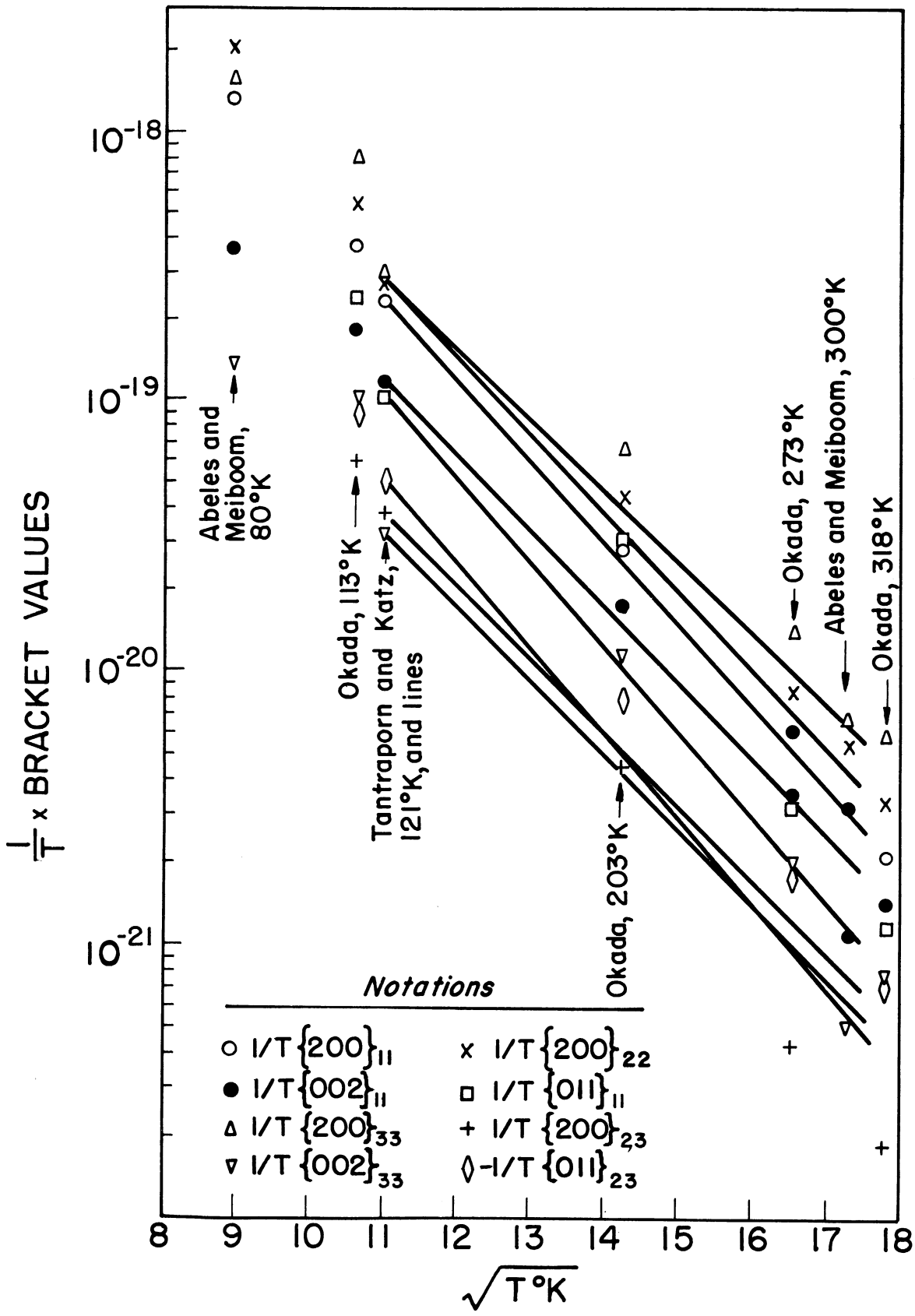

Fig. 5. Comparison of second-order brackets by various authors. Markers at $\sqrt{T}$ = 11 identify our lines.

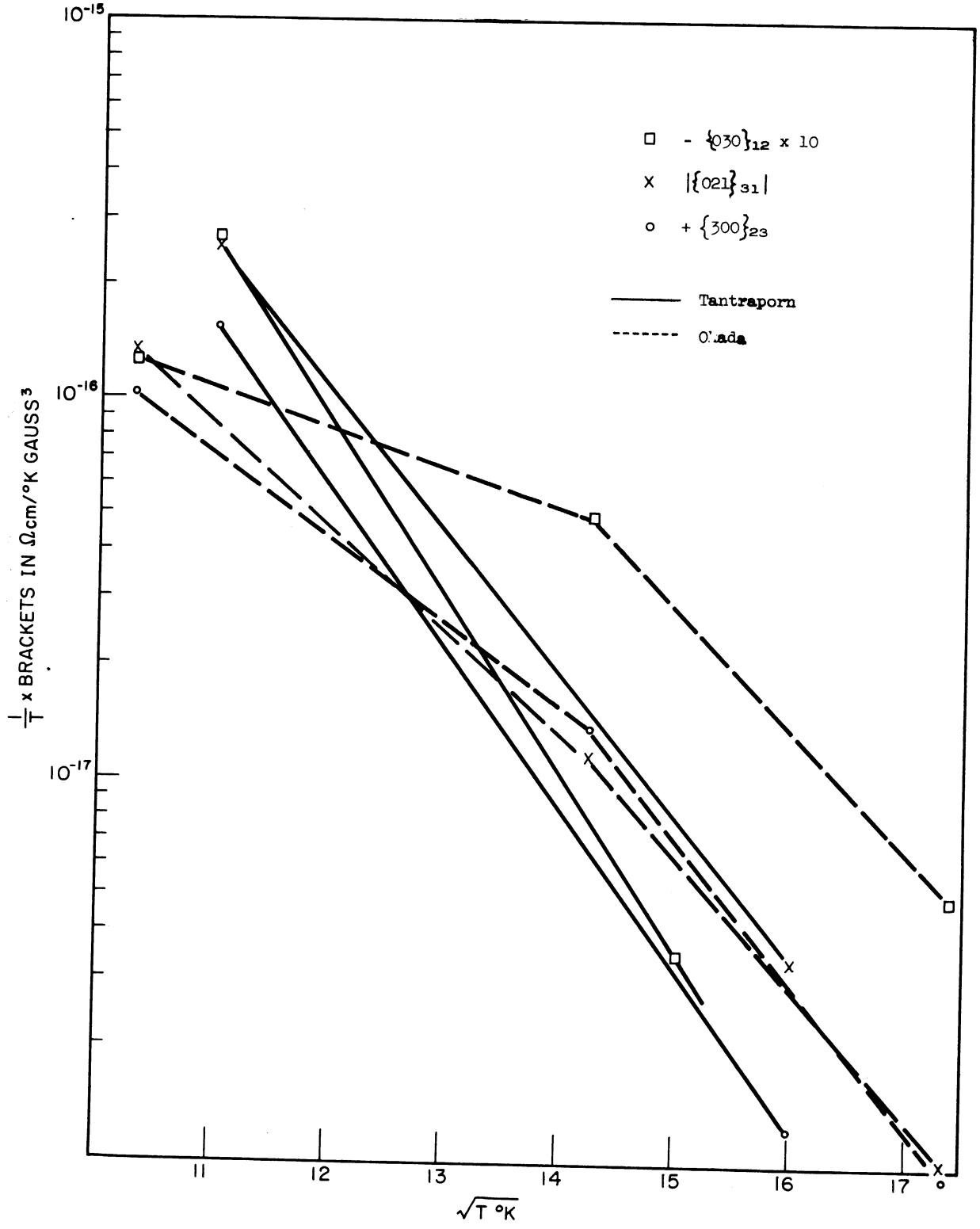

Fig. 6. Comparison of the third-order brackets.

first-order bracket, which is very small and sensitive, does not agree so well, but the discrepancy is not unreasonable. There is more marked disagreement among the second-order brackets. For the third-order brackets the experimental errors become larger and hence the disagreement is not so bad as for the second order. No literature exists with which to compare our higher order brackets.

The divergence of the results between various authors may be due to the different degrees of impurity and imperfection of the bismuth samples used. Various authors have either reported difficulties in reproducibility or have failed to check their data for internal check relations. For example, Connell and Marcus[12] and Babiskin[13] report that their galvano-magnetic measurements were not reproducible as a function of the temperature, between various runs. Okada[9] stated only one check between two samples, namely, two different measurements of $\rho_{11,11} = \{200\}_{11}$. Abeles and Meiboom[10] did not state any checks for their measurements. Our measurements satisfied all check relations involving quantities measured on one sample, indicating reproducibility; the check was not quite so good but still satisfactory for relations involving quantities derived from more than one sample (see Appendix 3). As mentioned earlier, this is probably due to slight differences of imperfections in the samples. Allowance for this has been made in the assignment, in Table VIII, of the values of $\Delta\Gamma$ and $\Delta\beta$.

3.7. CONCLUSIONS FOR BISMUTH

The experimental results of Table VIII suggest the following conclusions.

I. The temperature dependence of the form (10) fits the experimental results very well for all brackets measured ($n \leq 6$), for $120°K < T < 300°K$. It fits Blake's data from 80°K to 450°K and probably holds for T up to the melting point of bismuth, 544°K.

II. The values of β are approximately the same for brackets of the same order n. The mean value of β for each n is roughly given by

$$\beta_n = \frac{2n}{n+4} \quad . \tag{13}$$

The fit of this relation is shown in Fig. 7.

III. The order of magnitude of Γ for the brackets in these units goes down by a factor 10^{-3} with each unit increase of n. This indicates that the series expansion (5) may diverge for fields $> 10^3$ gauss at 120°K and 10^4 gauss at room temperature.

IV. As has been pointed out by Okada,[9] the longitudonal magneto-resistance is not always smaller than the transverse one. According to our Table VIII $\{200\}_{11} > \{002\}_{11}$, which implies that for a sample

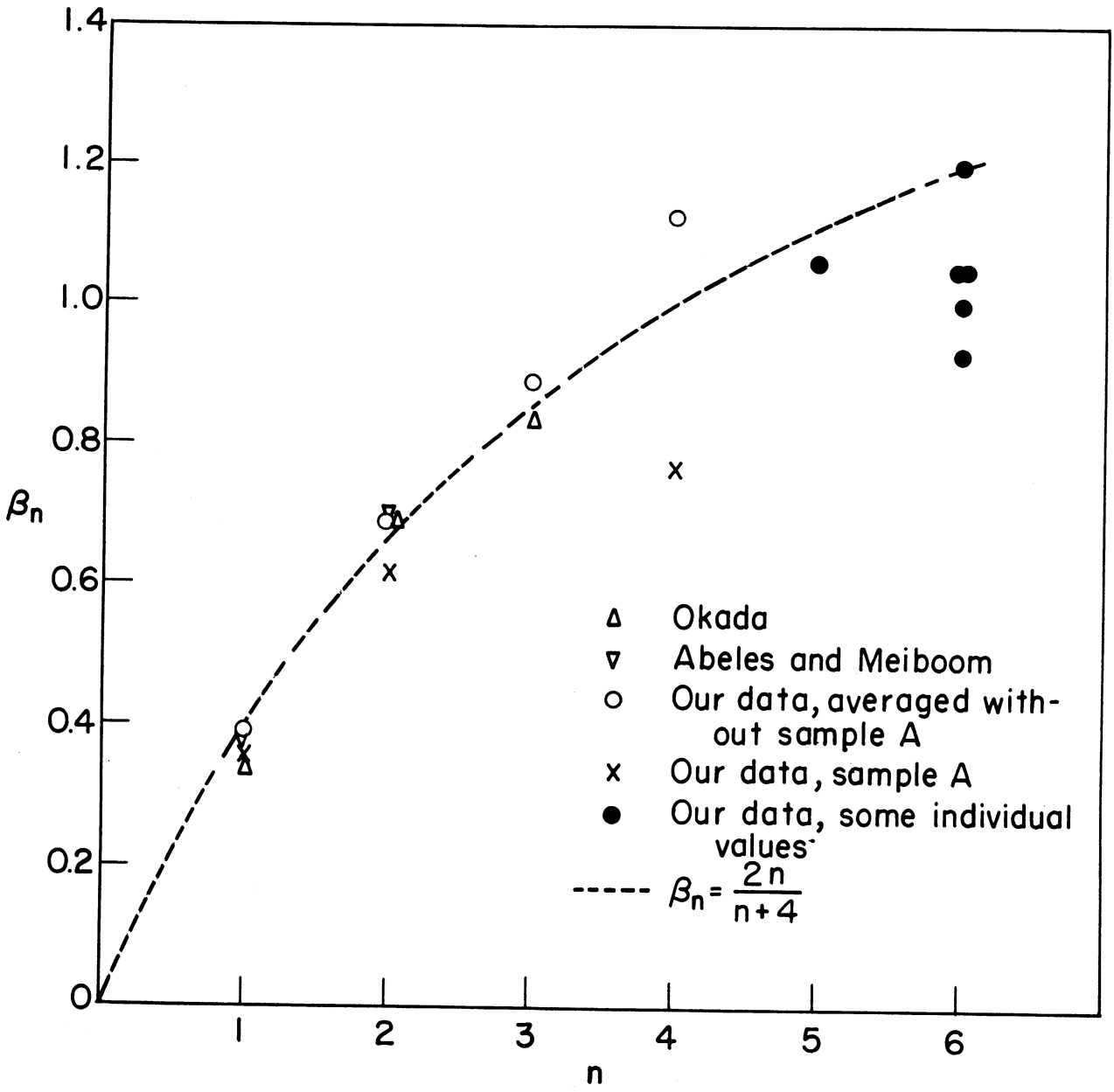

Fig. 7. The dependence of β_n on n.

with the binary axis along the rod, the longitudinal magneto-resistance is larger than this transverse. For a sample with the trigonal axis along the rod it is smaller. For small fields the magneto-resistance in bismuth is always positive.

V. The magnitudes of different brackets of the same order may differ by as much as a factor of a hundred. Measurements $\{001\}_{12}$ showed for some samples small negative values, though most samples gave positive values. Apparently this bracket is very close to zero and sensitive to the perfection of the crystal. The smallness of this Hall bracket is practically a proof for the occurrence in bismuth of electrons and holes as competing current carriers, as proposed, for example, in the two-band model of Jones.[14]

4. Analysis of Blom's Data for Gallium

4.1. INTRODUCTION

Blom[8] has taken measurements of single crystals of gallium, the results of which were published in 1950. Because our type of complete analysis was not available at that time, he did not provide measurements on a sufficient number of rightly oriented (grown) samples to permit the complete determination of all individual brackets involved. However, since his data are extensive and taken with care it seems worth while to translate his results into our bracket notation. The purpose of such a translation is to provide a basis for comparison between our rather unconventional findings for bismuth and independent data on some other anisotropic material such as gallium. For this type of translation it is necessary to carry out Fourier analyses of certain sets of his data, and proceed essentially as described in Section 3.5 for bismuth, with the difference that Table III is applicable instead of Table I since gallium belongs to the class D_2.

Since Blom's measurements are only of the magneto-resistance type, only even-order brackets can be determined. In practice the determinations are good for n = 2 and 4. The presence of higher-order terms is evident, in his data, especially at low temperatures and high magnetic fields. They have not been used for the determination of higher-order brackets because the errors involved would become relatively large, and this did not justify the disproportionate amount of labor involved.

The temperature range extended from 80°K down to 10.4°K with a few isolated runs above and below these limits. The crystals were rods grown along the (100), (010), (001), and (011) directions. We find that the temperature dependence of the brackets can be represented here just as in the case of bismuth by an expression of the form $\Gamma_0 \, T \, e^{-\beta \sqrt{T}}$ within the experimental error.

4.2. RESULTS

The values derived for the brackets of order 0, 2, 4 from Blom's work are given in Table IX. Because Blom's data are given relative to the resistance we write the coefficient in formula (10) as $\Gamma'_0 \rho_0$ instead of Γ_0. The resistivity at 0°C, ρ_0, was found to be isotropic within the experimental error by Blom and its value is given as $\rho_0 = 5.27 \times 10^{-5}$ Ω cm.

The brackets $\{031\}_{23}$ and $\{013\}_{23}$ cannot be solved for separately in terms of the measured quantities. The bracket $\{211\}_{23}$ cannot be obtained with reasonable accuracy from the available data.

4.3. CONCLUSIONS FOR GALLIUM

The results allow the following conclusions.

I. The temperature dependence of the form (10) fits the experimental results very well for all brackets measured ($n = 0,2,4$) for $10.4°K < T < 80°K$.

II. The values of β are approximately the same for brackets of the same n, although the spread is somewhat larger for gallium than for bismuth. The mean values are $\bar{\beta}_2 = 0.75$ and $\bar{\beta}_4 = 0.98$. This is again in rough agreement with the expression $\beta_n = 2n/(n+4)$ which takes the values 0.67 for $n = 2$ and 1.00 for $n = 4$. It seems, therefore, that the parameter β describes a feature of the temperature dependence which is independent of the material within certain limits.

III. The order of magnitude of Γ_0 goes down by a factor of 10^{-4} per unit of n. This corresponds to a factor of $10^{-4.5}$ for Γ_0, a value which is significantly larger than for bismuth. It indicates that, for gallium at room temperature, the series expansion (5) may have a radius of convergence of not less than 10^6 gauss.

IV. The equality, within experimental accuracy, of the three zero-order brackets (resistivities) is not required by symmetry and is therefore probably not an exact equality.

V. On the whole, therefore, the temperature dependence of the galvanomagnetic constants for gallium follows the same general pattern as for bismuth. Equation (10) seems to have more than casual importance.

TABLE IX

VALUES DERIVED FROM BLOM'S WORK FOR BRACKETS OF GALLIUM
ACCORDING TO $\{\ \} = \Gamma'_o\ \rho_o\ T\ e^{-\beta\sqrt{T}}$ ($\rho_o = 5.27 \times 10^{-5}\ \Omega$ cm)

Bracket	Γ'_o Gauss^{-2} °K^{-1}	β	$\Delta\Gamma'_o$ %
$\{000\}_{11} = \rho_o$	3.66×10^{-3}	0	3
$\{000\}_{22}$	3.66	0	3
$\{000\}_{33}$	3.66	0	3
$\{200\}_{11}$	16×10^{-11}	0.79	25
$\{020\}_{11}$	1.5	0.61	20
$\{002\}_{11}$	9.5	0.57	25
$\{200\}_{22}$	88	0.94	40
$\{020\}_{22}$	5.0	0.77	5
$\{002\}_{22}$	4.5	0.66	30
$\{200\}_{33}$	66	0.82	30
$\{020\}_{33}$	14	0.76	40
$\{002\}_{33}$	3.9	0.77	20
$\{011\}_{23}$	180	0.82	80
$\{400\}_{11}$	40×10^{-19}	1.51	100
$\{040\}_{11}$	1.3	0.80	80
$\{004\}_{11}$	6.3	0.78	80
$\{022\}_{11}$	71	0.88	90
$\{202\}_{11}$	3.8	0.67	40
$\{220\}_{11}$	105	1.06	50
$\{400\}_{22}$	5.7	0.93	60
$\{040\}_{22}$	9.4	1.24	10
$\{004\}_{22}$	1.4	0.81	40
$\{022\}_{22}$	24	1.19	30
$\{202\}_{22}$	20	1.04	90
$\{220\}_{22}$	3.3	0.98	30
$\{400\}_{33}$	13	0.89	60
$\{040\}_{33}$	2.1	0.89	40
$\{004\}_{33}$	2.3	1.01	90
$\{022\}_{33}$	21	1.08	100
$\{202\}_{33}$	24	0.94	30
$\{220\}_{33}$	64	1.02	30

5. Electron Theoretical Considerations

5.1. STATEMENT OF PROBLEM

The problem is to derive relevant features of the Fermi surface, or of the energy surfaces $E(\vec{k})$ in general, from the data collected experimentally. This is a difficult task for which the solution is not yet available. A somewhat simpler task is to assume a model for $E(\vec{k})$ and check whether this is compatible with all the results. The obviously simplest way is to assume $t = t(E)$ (or $t =$ constant if one simplifies to the extreme) and to take for $E(\vec{k})$ a quadratic form. The most general quadratic form which is compatible with the symmetry of bismuth has been introduced by Shoenberg.[15] The energy surface is made up of three identical ellipsoids, rotated by 120° about k_3, one of which is expressed by

$$E(\vec{k}) = \alpha_{11}k_1^2 + \alpha_{22}k_2^2 + \alpha_{33}k_3^2 + 2\alpha_{23}k_2k_3 \qquad (14)$$

where k_1, k_2, k_3 are the symmetry coordinates defined earlier, now referring to wave number space. In addition, Shoenberg assumed a hole band of revolution about k_3

$$E(\vec{k}) = \beta_{11}(k_1^2 + k_2^2) + \beta_{33}k_3^2 \qquad (15)$$

According to Kao,[2] in the multiband (or multivalley) theory without interband scattering, one has for the conductivity brackets in terms of an integral in k- or wave number space:

$$[m\text{-}p,\ p,\ n\text{-}m]_{ij} = ab^n \iiint \delta\left(\frac{\partial E}{\partial k_i}\right) P\{(t\Omega_1)^{m-p}\ (t\Omega_2)^{p}\ (t\Omega_3)^{n-m}\}\ \left(t\frac{\partial E}{\partial k_j}\right)dk_1dk_2dk_3 \qquad (16)$$

where

$\delta = -\frac{\partial f_o}{\partial E}$

f_o = the Fermi distribution function

E = energy

$a = e^2/4\pi^3\hbar^2$

$b = \frac{e}{\hbar^2 c}$

e = charge of the carrier (including the sign)

c = light velocity

t = relaxation time (assumed to exist)

Ω = $-\nabla E \times \nabla$

P{ } stands for the sum of all permutations of (m-p) operators $t\Omega_1$, p operators $t\Omega_2$, and (n-m) operators $t\Omega_3$, in different order. This sum consists of n!(m-p)! p!(n-m)! terms.

For s noninteracting bands, the total conductivity bracket is the sum of the contributions of this form from all bands.

Thus a first task seems to be the finding of the best fit to our data for the six parameters α_{11} α_{22} α_{33} α_{23} β_{11} β_{33} and to see what values of the Fermi energy E_F (implicit in f_0) and what functional form of t(E) are required to fit the experimental temperature dependence. This analysis turned out to be more than we could handle in the time available. While work is being continued, we are reporting here what has been achieved, and along what lines results can be expected.

5.2. METHOD OF ATTACK

The solution of our problem is not merely a matter of finding a best fit. The situation is more intricate, because the assumptions made at the start to make the calculations tractable at all, such as the ellipsoidal energy surfaces, are not the most general, compatible with symmetry requirements. Thus the problem is to be attacked in three steps. The first step will now be described.

The effect of the choice of the model is to introduce further dependences among the brackets, which are independent of the values to which the parameters will be adjusted for best fit. To judge the usefulness of a model, it is therefore necessary first to check whether our data agree, or at least do not conflict, with such dependences. The labor involved in establishing these dependences is considerable, and increases rapidly with increasing order n of the brackets. After these dependences have been completely established and checked, experimental results have to be adjusted within the tolerances listed, to agree exactly with these. The next (second) step is then the adjustment as far as possible of the parameters. It turns out that, without reference to the unknown function t(E), it is relatively easy to adjust the parameter ratios, but the adjustment of their scaling factor is coupled with the question whether a function t(E) can be found that will produce, within experimental error limits, the dependence (10) on the temperature. The third stage consists of finding the function t(E) and the scaling factor. At the time of writing this report, we are still in the first stage of completing the dependences introduced by the model.

5.3. RESULTS

The results are obviously of crucial importance because they decide whether the model hitherto most recommended for bismuth is adequate or not for the description of galvano-magnetic effects. It would therefore not be proper to communicate here preliminary unfinished results. It is our intention to finish this line of inquiry in the course of time and publish the results when they are complete and properly checked.

However, we have not encountered fundamental inadequacies of the model up to the point to which our analysis has progressed, namely, up to n = 2. The effective masses of electrons and holes follow the general trend of the literature without, however, agreeing quantitatively. Our effective mass differences in the principal directions are large but not quite as large as reported in the literature.

5.4. A SPECIAL FEATURE

One can inquire whether Eq. (16), without any further assumption except that $t = t(E)$, in particular without any assumption about $E(\vec{k})$ other than that it comply with symmetry requirements, is rich enough to account for galvano-magnetic data in general.

If Eq. (16) would lead to an equal number of independent brackets as the phenomenological theory, it would be rich enough, but it also would be no theory to speak of, for it would simply replace an empirical description with an infinite number of parameters by a model description with an equally large number of parameters.

The model theory becomes the more valuable the more additional dependences it predicts among the empirical brackets, provided these are verified by experiment. Consequently, it is desirable to investigate which additional dependences, if any, are generated by the model before special forms of $E(\vec{k})$ are introduced.

A certain amount of preliminary progress has been made in this direction, but again time limitation has precluded reaching a stage worth reporting. The presence of theoretical extra relations has been discovered for temperatures, low compared to the Fermi temperature, as a special feature in this investigation. Since, however, the accepted Fermi temperature of bismuth lies below our experimental temperature range, we are not in a position to check them. However, the existence of such a relation and indications for the existence of other ones is considered a significant new feature.

5.5. CONCLUSIONS OF THE ELECTRON THEORETICAL PART

The work on the electron theoretical interpretation of galvano-magnetic data has brought into focus a number of new questions which precluded finishing

the theoretical discussion of our results, but at the same time opened up new and promising avenues for further research into some of the basic features of the galvano-magnetic effects. As a result of this state of affairs, every conclusion can be phrased in a negative as well as in a positive way.

Ia. The comparison of the experimental brackets and their temperature dependence with Shoenberg's model has not been carried out beyond a partial comparison up to the second order, which produced no conflicts so far.

Ib. In comparing the experimental brackets at one temperature with Shoenberg's model, it was discovered that this model must predict a series of new relations between the brackets in addition to the relations due to symmetry regardless of the choice of the function t(E). The establishing of such relations was started.

IIa. The question of comparison of the temperature dependence between experiment and Shoenberg's theory depends on finding a suitable function t(E) for the relaxation time. The existence of a suitable function so far is unknown.

IIb. It was discovered that the assumption of the existence of a suitable function t(E) leads to additional theoretical bracket relations even if the energy surfaces are not restricted to ellipsoids as in Shoenberg's theory. The establishing of such relations was started.

It can be expected that, when the theoretical relations mentioned in Ib and IIb are established, a much more significant manner of comparing theory and experiment will result, which not only is able to register agreement or disagreement but also will point to any particular assumption in the theory causing disagreement. In particular, a distinction is in prospect between consequences of a too simple shape of the energy surfaces and consequences of a too simple form of the relaxation time function.

APPENDIX 1

ASSIGNMENT OF SYMMETRY COORDINATE AXES IN BISMUTH

Bismuth belongs to the rhombohedral class, having two face-centered almost cubic lattices displaced with respect to each other almost by half of body diagonal, with each cubic lattice being a little stretched along the diagonal. The amounts of displacement and stretch, expressed as fractions of a space diagonal of a perfect cube, are 0.0621 and 0.0346, respectively. The rhombohedral unit vector is 4.74Å.

The third symmetry coordinate axis, k_3, is chosen along the body diagonal, an axis of threefold rotational symmetry. It is immaterial which of the two opposite senses is chosen as the positive k_3 axis.

Perpendicular to k_3 the crystal has three binary axes of symmetry making angles of 120° with each other. The choice of the positive directions of the binary axes, once the positive direction of the trigonal axis is fixed, must be definite, as otherwise one would have hexagonal symmetry. This choice can be made in two ways, which can be distinguished experimentally as follows.

If an actual crystal is cleaved along the basal trigonal (perfect) plane and along the three imperfect planes, a pyramidal point may result. This pyramidal point may in principle be on either side of the perfect plane. We choose to draw it on that side of the perfect plane which is indicated by the positive choice of $\vec{k}_3$.

Figure 8 shows the pyramidal point on one side of the perfect plane. $\vec{AB}$, $\vec{AC}$, and $\vec{AD}$ are the rhombohedral unit vectors, BCD is the trigonal (perfect) plane, and $\vec{OA}$ lies along the chosen positive direction of k_3. Let the outward normal of an imperfect plane be given by a unit vector $\vec{\xi}$. Then we define the positive direction of the binary axis to be along $\vec{\xi} \times \vec{k}_3$. This definition defines uniquely positive directions for the three binary axes, regardless of the side of the perfect plane on which $\vec{OA}$ is taken, since $\vec{\xi}$ reverses with the reversal of $\vec{k}_3$, leaving $\vec{\xi} \times \vec{k}_3$ invariant.

The symmetry coordinate axis k_1 is now chosen along one of the three positive senses of the binary axes. The axis k_2 then is added to form a right-hand triad with k_1 and k_3.

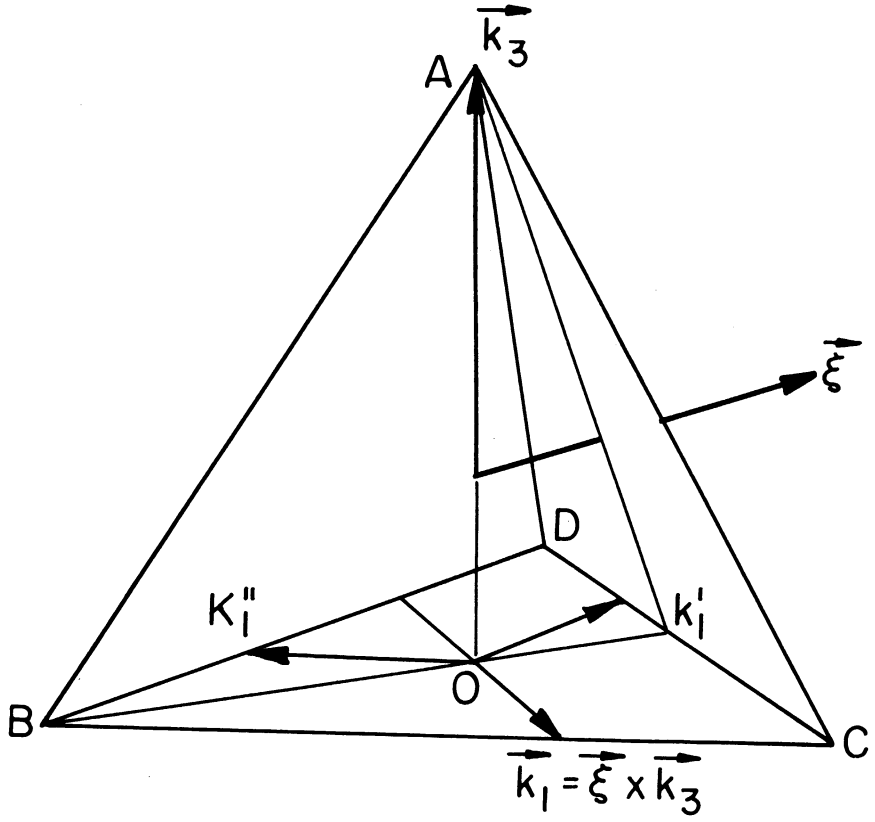

Fig. 8. Assignment of symmetry coordinate axes in bismuth.

The need for a careful definition of a positive sense along the binary axes was apparently not recognized by previous workers. It is not clear from the literature whether the positive k_1 direction of Okada, for example, corresponds to the above definition or its opposite. If another investigator chooses the opposite sense of k_1 as positive, the result will be that, although he also uses a right-hand system of coordinates, some galvano-magnetic brackets defined relative to his system differ by a minus sign from ours. This sign difference occurs if and only if this bracket depends on k_3 to an odd power. (In judging the power, one must take into account that $\vec{B}$ is really an antisymmetric tensor of the second rank. Thus, for example, $[001]_{12} \rightarrow [(23)^0\ (31)^0\ (12)^1]_{12}$ contains k_3 to the power zero, hence is independent of the above subtlety, while $[011]_{11} \rightarrow [(23)^0\ (31)^1\ (12)^1]_{11}$ contains k_3 to the power one; hence its sign is dependent on the above definition.)

Summarizing the results of this analysis, we can state the following.

1. For an arbitrary choice of the positive sense of k_3, there is an ambiguity for the choice of the positive sense of k_1 along a binary axis,

2. We adopt the convention $\vec{k}_1 = \vec{\xi} \times \vec{k}_3$ where $\vec{\xi}$ is the outward normal unit vector of an imperfect cleavage plane with respect to the pyramid of cleavage planes.

3. The signs of all our brackets are uniquely defined in this system. This scheme is self-consistent in that if k_3 is reversed, k_1 remains, k_2 reverses, and since k_1 lies along a binary axis, the brackets remain invariant (see Kao,[5] corollary I).

4. If the convention 2 is replaced by $\vec{k}_1 = -\vec{\xi} \times \vec{k}_3$, most brackets remain invariant but some change sign. The latter are marked with an asterisk in Table VIII. This sign ambiguity must be allowed for when comparing results of different authors, insofar as the manner in which the positive sense of k_1 is chosen is not stated explicitly.

APPENDIX 2

ANGLES

To specify the orientations of the electric and magnetic field and of the current with respect to the crystal axes, two coordinate systems are used.

(1) The symmetry coordinates $k_i (i = 1, 2, 3)$:

k_3 along the trigonal axis. Arbitrary choice of positive sense.
k_1 along a binary axis. Positive sense according to Appendix 1.
k_2 accordingly to make a right-hand triad.

(2) The laboratory coordinates $X^\alpha (\alpha = 1, 2, 3)$:

X^1 along the length direction of the sample. Positive sense making an angle of not more than 90° with $+k_3$.
X^2 along the horizontal direction connecting the Hall probes which is also the direction of one of the mechanical rotation axes. Positive sense chosen arbitrarily.
X^3 accordingly to make a right-hand triad.

The two coordinate systems can be related to each other by means of three angles, Θ, κ, α:

Θ = angle between X^1 and k_3, always positive and not more than 90°.
κ = angle measured from the vector $\vec{k}_3 \times \vec{X}^1$ to k_1; the positive sense corresponds to an advance along $+k_3$ according to a right-hand screw.
α = angle measured from X^2 to $\vec{k}_3 \times \vec{X}^1$; the positive sense corresponds to an advance along $+X^1$ according to a right-hand screw.

The direction cosines between the two sets of coordinate axes, l_i^α, can be expressed in terms of the angles Θ, κ, α.

$$l_1^1 = \sin\Theta \sin\kappa \qquad l_2^1 = -\sin\Theta \cos\kappa \qquad l_3^1 = \cos\Theta$$

$$l_1^2 = \cos\alpha \cos\kappa + \sin\alpha \sin\kappa \cos\Theta \qquad l_2^2 = -\cos\alpha \sin\kappa + \sin\alpha \cos\kappa \cos\Theta \qquad l_3^2 = -\sin\alpha \sin\Theta$$

$$l_1^3 = -\sin\alpha \cos\kappa + \cos\alpha \sin\kappa \cos\Theta \qquad l_2^3 = -\sin\alpha \sin\kappa + \cos\alpha \cos\kappa \cos\Theta \qquad l_3^3 = \cos\alpha \sin\Theta$$

To express the direction of the horizontal magnetic field $\vec{B}$ with respect to the laboratory coordinate axes, the angles ψ, ϕ are defined as follows:

ψ = angle measured from the downward vertical to X^1; the positive sense corresponds to an advance along X^2 according to a right-hand screw.

ϕ = angle measured from $\vec{B}$ to X^2; the positive sense corresponds to an advance along the downward vertical according to a right-hand screw.

The direction cosines γ_i of the magnetic field $\vec{B}$ with respect to the symmetry coordinate axes are then

$$\gamma_1 = -\sin\phi(\sin\psi\sin\theta\sin\kappa - \cos\psi\sin\alpha\cos\kappa + \cos\psi\cos\alpha\cos\theta\sin\kappa) + \cos\phi(\cos\alpha\cos\kappa + \sin\alpha\sin\kappa\cos\theta)$$

$$\gamma_2 = -\sin\phi(\sin\psi\sin\theta\cos\kappa + \cos\psi\sin\alpha\sin\kappa + \cos\psi\cos\alpha\cos\theta\cos\kappa) - \cos\phi(\cos\alpha\sin\kappa - \sin\alpha\cos\kappa\cos\theta)$$

$$\gamma_3 = \sin\phi(\sin\psi\cos\theta - \cos\psi\cos\alpha\sin\theta) + \cos\phi\sin\alpha\sin\theta.$$

Substitution of the proper values of θ and κ for the samples, as described in Table IV, and the proper values of α and ψ for the settings, as described in Table V, permit direct verification (by means of the above relations) of the statements made in Section 3.5 concerning the method of separation of the brackets resulting in Tables VI, and VII. For further details and worked out examples, the reader is referred to Ref. 3.

The mechanical construction by means of which the angles ϕ, ψ, and α were varied is partially visible in Fig. 1. The ϕ rotation turns the entire sample holder around a vertical axis. It was motor-driven at a slow rate of about one revolution in 4.5 min. It could turn clockwise and counterclockwise, thus allowing the elimination of "dynamo effect" (induced emf due to rotation in the magnetic field). The ψ rotation turns about the horizontal axis which can clearly be seen in Fig. 1. It was set for a given value for each run by means of a suitable train of gears, manipulated from outside of the clear Dewar cryostat in which the sample and holder were immersed. The α rotation would turn the sample about its longitudinal axis and was likewise set for each run. The gear connections for this setting are only partially visible in Fig. 1. The line connecting the Hall probe contact points remained always parallel to the horizontal ψ axis.

APPENDIX 3

EXAMPLES OF DATA ANALYSIS

The following example illustrates the method of separation and determination of the brackets. From measurements on sample A, setting 1 (see Tables IV and V for specifications), a curve with the magneto-resistance as a function of the angle ϕ is obtained at a given temperature T and a given magnetic field B. Fourier analysis yields among other things the constant ${}^{1A}C_0$ [see Eq. (8)]. According to Eq. (3) in Table VI, this is equal to $B^4 \{400\}_{33} + B^2\{200\}_{33}$. Repetition for various values of T and B permits plotting of log $1/T\ {}^{1A}C_0$ versus $\sqrt{T}$ for various values of B, as shown in Fig. 9. The points lie on almost straight lines. The fact that each bracket would yield a straight line does not mean that their linear combinations as plotted here must lie on a straight line. The almost straight graphs indicate that the second-order term here greatly outweighs the fourth-order terms, suggesting that higher-order terms are completely negligible.

From the graphs of Fig. 9, points are taken off at various values of $\sqrt{T}$, replotting $1/TB^2\ {}^{1A}C_0$ versus B^2 in Fig. 10. According to the equation mentioned, the intercept and slope of these lines (each referring to a constant temperature as a parameter) represents $1/T\ \{200\}_{33}$ and $1/T\ \{400\}_{33}$, respectively. In Figs. 11 and 12 these quantities are plotted logarithmically versus $\sqrt{T}$. The results show the linear dependence according to Eq. (10), and permit the determination of Γ_0 and β for both brackets individually. This completes the task for these brackets. The other brackets were determined by analogous handling. In a few instances the presence of sixth-order terms is indicated and their evaluation follows similar lines.

It was stated that the equations of Tables VI and VII were used for the determination of the brackets, but that more equations were available and were used as check relations. Actually, in our work there are 22 possible check relations, of which 9 are trivial, leaving 13 genuine check relations among the measured quantities. A complete list of these is given by Tantraporn.[3] As an example we consider one of them here:

$$ {}^{1C}C_0 + {}^{1C}C_2 \cos 2\,{}^{1C}\phi_2 + {}^{1C}C_4 \cos 4\,{}^{1C}\phi_4 = {}^{2C}C_0 + {}^{2C}C_2 \cos 2\,{}^{2C}\phi_2 + {}^{2C}C_4 \cos 4\,{}^{2C}\phi_4 $$

Figure 13 shows that this relation is satisfied within experimental limits and the same was found of the other 12. This feature gives considerable reliability to our data. It must be pointed out that the check relation taken above as an example involves only quantities from one sample (C) for different settings (1 and 2). This type of check tells something only about the accuracy of settings and of the analysis of data. Some of the check relations, however, involve more than one sample. In that case, somewhat larger errors were apparent but the overall agreement was not unsatisfactory (see for example, Fig. 3).

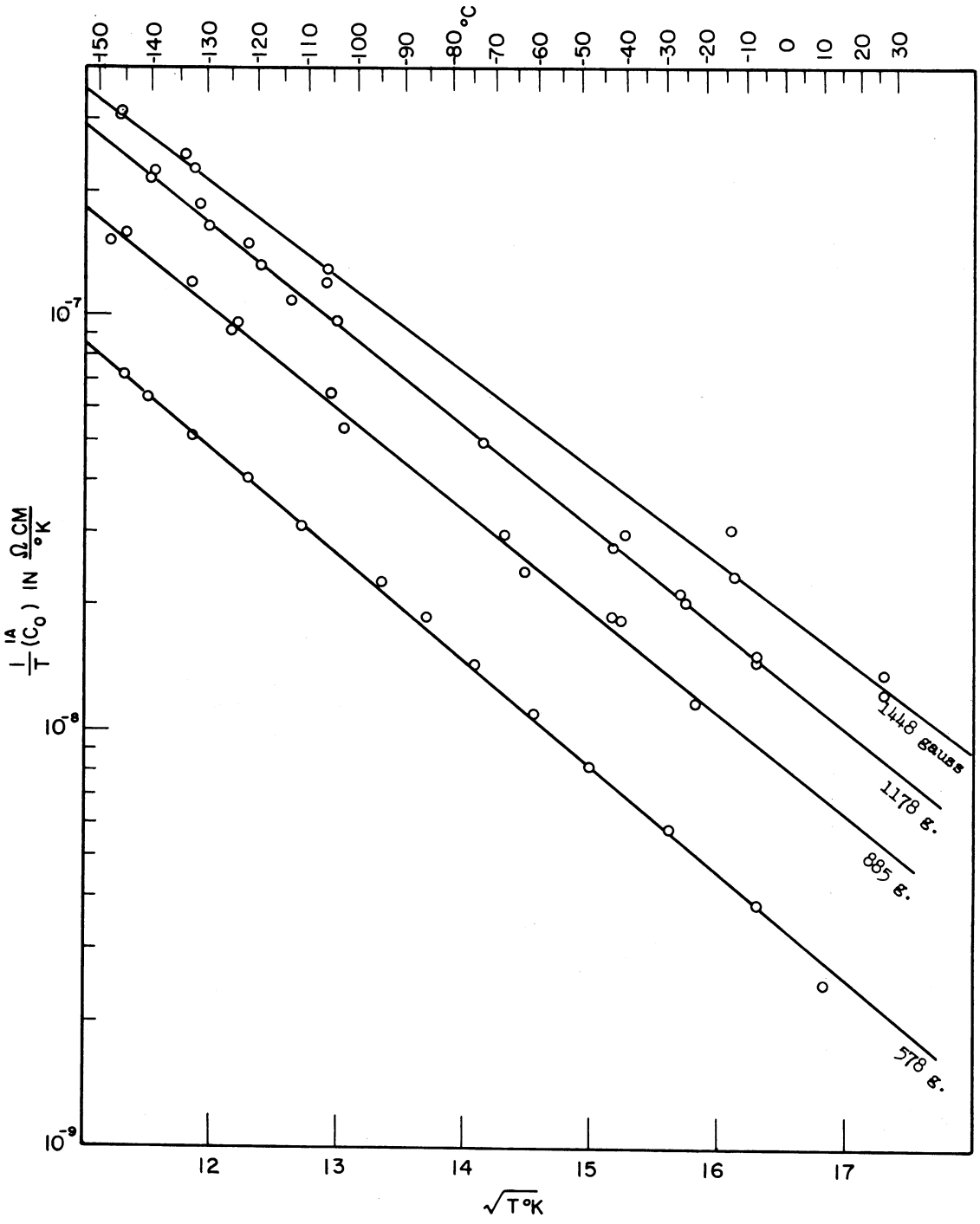

Fig. 9. $1/T\ {}^{1A}C_o$ vs $\sqrt{T}$ for various values of the magnetic field.

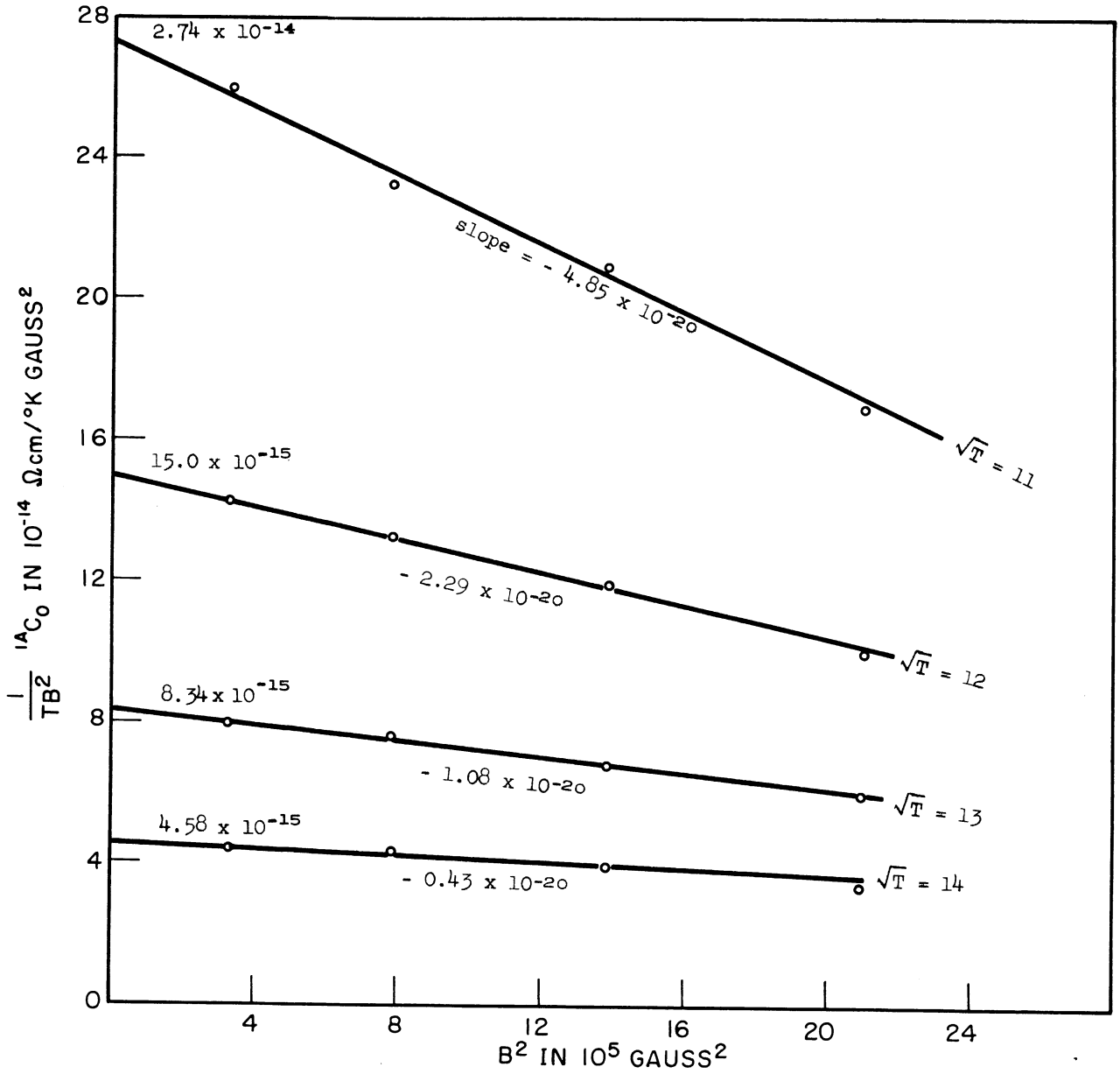

Fig. 10. Separation of the second- and fourth-order brackets as intercepts and slope, respectively. $\sqrt{T}$ = 15, 16, 17 lines are omitted.

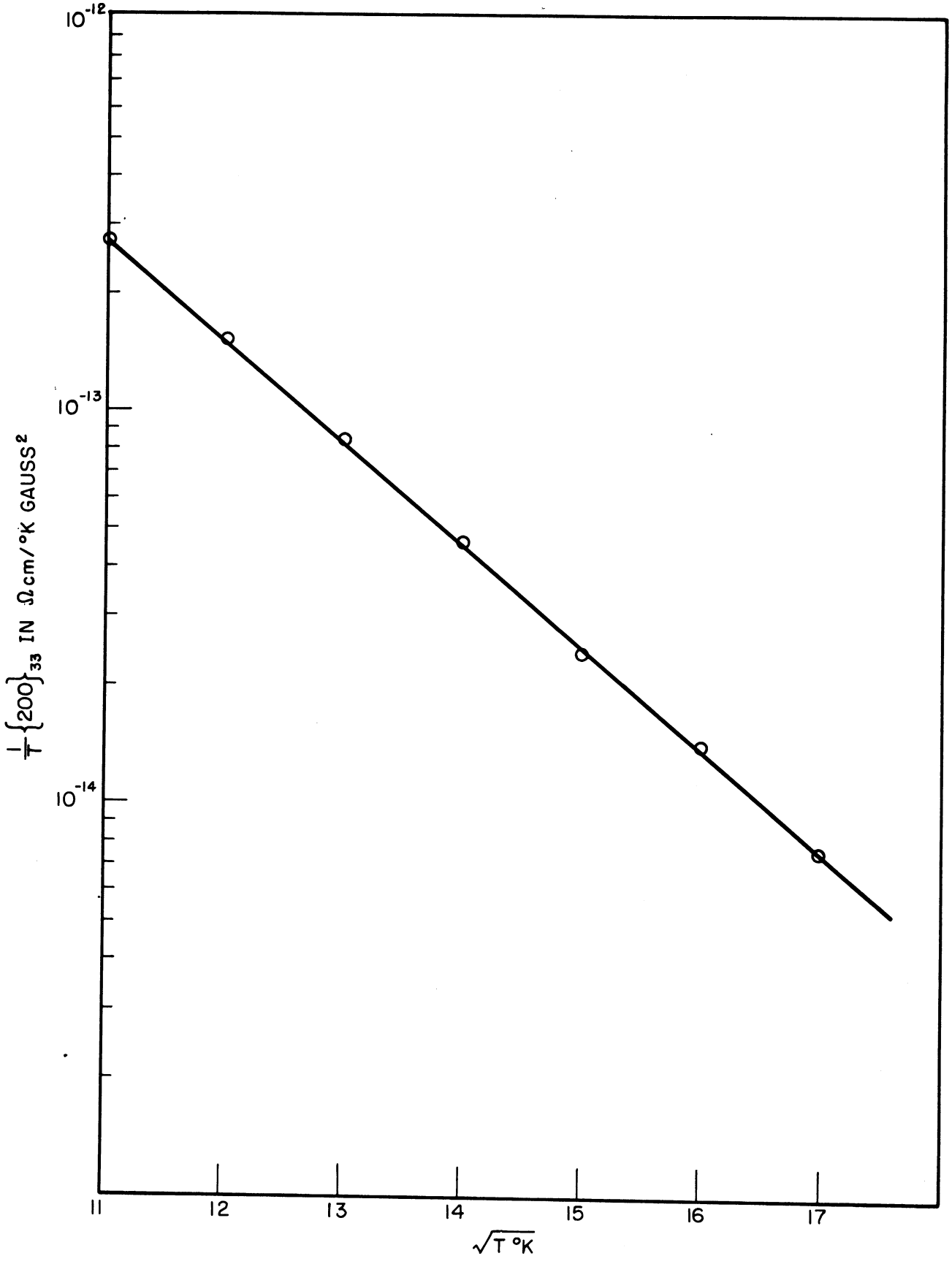

Fig. 11. $1/T\ \{200\}_{33}$ versus $\sqrt{T}$ from intercepts of Fig. 10.

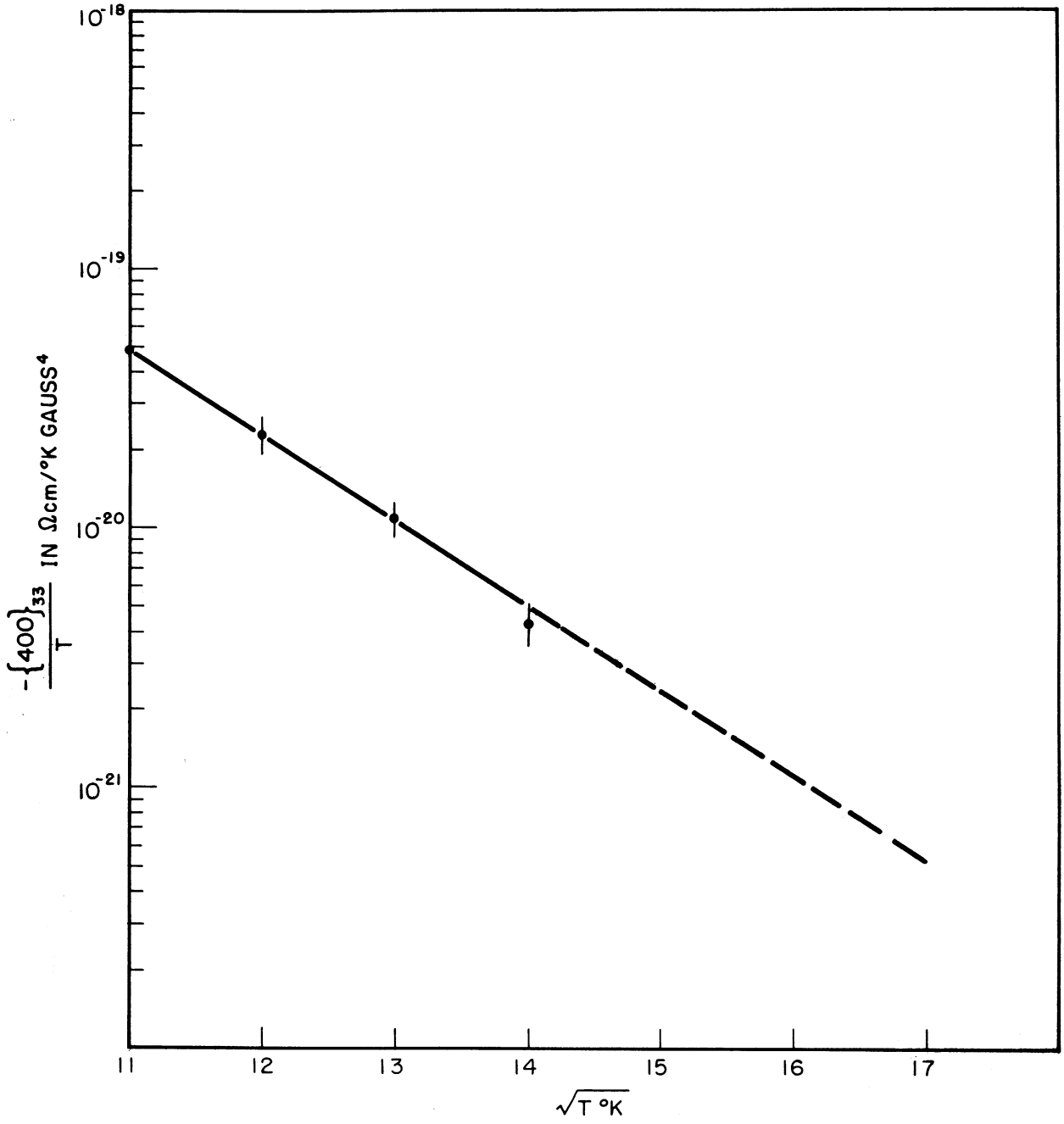

Fig. 12. $-1/T\ \{400\}_{33}$ versus $\sqrt{T}$ from slopes of Fig. 10.

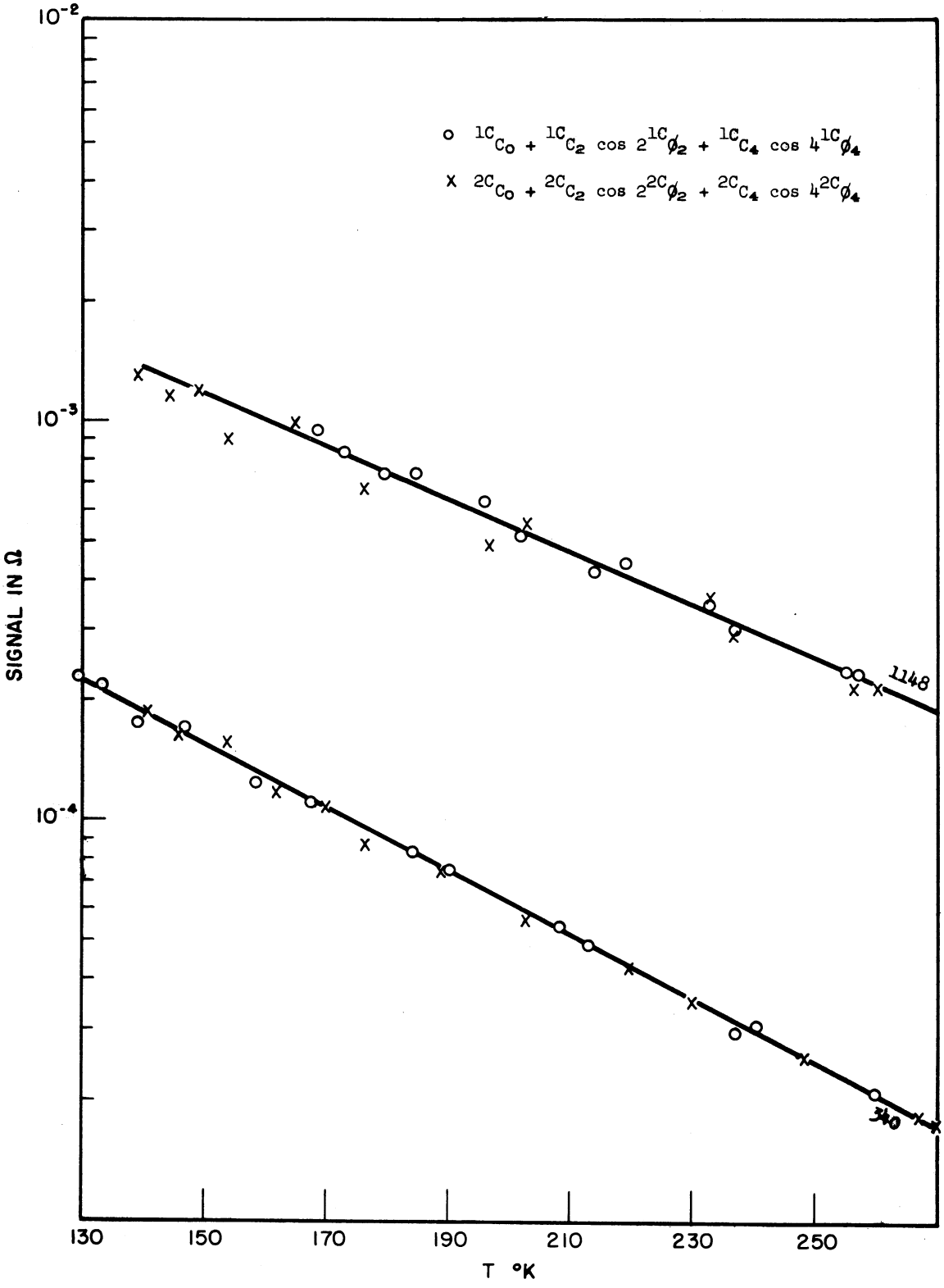

Fig. 13. Check relation for sample C.

REFERENCES

1. G. B. Spence, An Investigation in the Zone Theory of the Energy of Electrons in Metals, Ph.D. thesis, Univ. of Mich., 1956; or: U.S. Air Force, Air Research and Development Command, Contract AF 18(600)-750, E.O. No. 670-729-BR-1, Project No. R-355-40-10, August, 1956 (Technical Report).

2. L. P. Kao, Theory of Isothermal Galvano Magnetic Effects for Single Crystals, Ph.D. thesis, Univ. of Mich., 1956.

3. W. Tantraporn, Measurement of the Phenomenological Galvano Magnetic Constants of Bismuth Single Crystals up to the Fourth Order of the Magnetic Field, and Their Temperature Dependence, Ph.D. thesis, Univ. of Mich., 1958.

4. L. P. Kao and E. Katz, "Phenomenological Theory of Anisotropic Isothermal Galvano Magnetic Effects," J. Phys. Chem. Solids, 6, 223 (1958).

5. R. L. Martin, Results of Investigation of Low Intensity Reciprocity Law Failure, Ph.D. thesis, Univ. of Mich., 1956; or U.S. Air Force, Air Research and Development Command, Contract No. AF 18(600)-750, E.O. No. 670-729-BR-1, Project No. R-355-40-10, August, 1956.

6. J. H. Enns and E. Katz," Photographic Sequence Exposure Experiment," J. Opt. Soc. Am., 47, 758 (1957).

7. Abstracts: E. Katz and L. P. Kao, "Note on Magneto Resistance," Phys. Rev., 94, 1433 (1954);

   E. Katz and L. P. Kao, "Theory of the Anisotropy of Magneto Resistance for Single Crystals," Phys. Rev., 98, 1534 (1955);

   E. Katz, J. H. Enns, and R. L. Martin, "Sequence Experiment for the Study of the Reciprocity Law Failure at Low Intensities," Phys. Rev., 98, 1556 (1955).

   E. Katz, 'Photographic "Order Principle,"' Phys. Rev., 98, 1556 (1955);

   E. Katz, R. L. Martin, and J. H. Enns, "Low Intensity Reciprocity Law Failure for Pure AgBr Emulsions of Different Grain Sizex," Phys. Rev., 98, 1557 (1955).

   E. Katz and J. H. Enns, "Photographic Emulsion Studies by the Sequence Exposure Experiment," Bull. Am. Phys. Soc., 3, 100 (1958).

8. J. W. Blom, Magneto Resistance for Crystals of Gallium, The Hague, M. Nÿhof, 1950.

9. E. van Everdingen, Comm. Leiden, No. 58 (1900);
F. C. Blake, Am. Physik, 28, 449 (1909);
T. Okada, J. Phys. Soc. Japan, 12, 1327 (1957).

10. B. Abeles and S. Meiboom, Phys. Rev., 101, 544 (1956).

11. A. H. Wilson, The Theory of Metals, Univ. Press, Cambridge (1953).

12. R. A. Connell and J. A. Marcus, Phys. Rev., 107, 940 (1957).

13. J. Babiskin, Phys. Rev., 107, 981 (1957).

14. H. Jones, Proc. Roy. Soc., A155, 653 (1936).

15. J. S. Dhillon and D. Shoenberg, Phil. Trans. Roy. Soc., A248, 1 (1955).

DISTRIBUTION LIST

No. of Copies		Agency
5		Commander Hq, AF Office of Scientific Research ATTN: SRQB Washington 25, D.C.
4		Commander Wright Air Development Center ATTN: WCRRH ATTN: WCRRL ATTN: WCRTL ATTN: WCRTM-1 Wright-Patterson Air Force Base Ohio
2		Commander Air Force Cambridge Research Center ATTN: Technical Library ATTN: CRRF L. G. Hanscom Field Bedford, Massachusetts
1		Commander, Rome Air Development Center ATTN: Technical Library Griffiss Air Force Base Rome, New York
1		Director, Office for Advanced Studies Air Force Office of Scientific Research P.O. Box 2035 Pasadena 2, California
1	(Inner Envelope— No Postage)	Commander European Office, ARDC c/o American Embassy Brussels, Belgium
	(Outer Envelope— bearing sufficient postage for delivery to Washington)	Superintendent Diplomatic Pouch Rooms Department of State Washington 25, D.C.

DISTRIBUTION LIST (Continued)

No. of Copies	Agency
10	Document Service Center Armed Services Technical Information Agency Arlington Hall Station Arlington 12, Virginia
2	Department of the Navy Office of Naval Research ATTN: Code 423 ATTN: Code 421 Washington 25, D.C.
1	Commanding Officer Naval Radiological Defense Laboratory San Francisco Naval Shipyard San Francisco 24, California
1	U. S. Atomic Energy Commission Library Branch Technical Information Division, ORE P.O. Box E Oak Ridge, Tennessee
1	Brookhaven National Laboratory ATTN: Research Library Upton, Long Island, New York
1	Argonne National Laboratory ATTN: Librarian P.O. Box 299 Lemont, Illinois
1	Knolls Atomic Power Laboratory ATTN: Document Librarian P.O. Box 1072 Schenectady, New York
1	National Science Foundation 1520 H Street, N. W. Washington 25, D.C.
1	Director of Research and Development Headquarters, United States Air Force ATTN: AFDRD-RE-3 Washington 25, D.C.
1	Officer in Charge Office of Naval Research Navy No. 100 Fleet Post Office New York,New York
1	Director, Research and Development Division General Staff Department of the Army Washington 25, D.C.
1	Division of Research U. S. Atomic Energy Commission 1901 Consititution Avenue, N. W. Washington 25, D.C.
1	Oak Ridge National Laboratory ATTN: Central Files Post Office Box P Oak Ridge, Tennessee
1	Ames Laboratory Iowa State College P.O. Box 14A, Station A Ames, Iowa
1	National Bureau of Standards Library Room 203, Northwest Building Washington 25, D.C.
1	Office of Technical Services Department of Commerce Washington 25, D.C.

DISTRIBUTION LIST (Concluded)

No. of Copies	Agency
1	Director, Office of Ordnance Research Box CM, Duke Station Durham, North Carolina
1	National Advisory Committee for Aeronautics 1512 H Street, N. W. Washington 25, D. C.
1	Document Custodian Los Alamos Scientific Laboratory P.O. Box 1663 Los Alamos, New Mexico
1	Arnold Engineering Development Center ATTN: Technical Library P.O. Box 162 Tullahoma, Tennessee
1	Commander Western Development Division (ARDC) ATTN: WDSIT P.O. Box 262 Inglewood, California
1	Commanding Officer Ordnance Materials Research Office Watertown Arsenal Watertown 72, Massachusetts
1	Commanding Officer Watertown Arsenal Watertown 72, Massachusetts ATTN: Watertown Arsenal Laboratories Technical Reports Section